A-63-4-3

Westinghouse

ELECTRIC CORPORATION

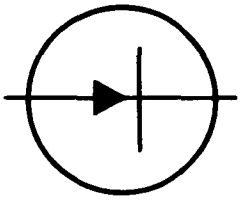

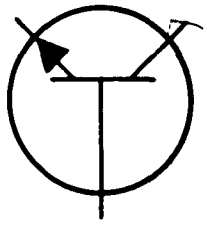

WESTINGHOUSE ELECTRIC CORPORATION
3001 Walnut Street
Philadelphia 4, Pennsylvania

Production Engineering Measure
Type 2N1016B Silicon Alloy Transistor

QUARTERLY PROGRESS REPORT NO. 3
Covering period through March 31, 1963

Contract No. DA-36-039-SC-86743
Order No. 19065-PP-62-81-81

Placed by
U. S. ARMY ELECTRONICS MATERIEL AGENCY
225 South Eighteenth Street
Philadelphia 3, Pennsylvania

Production Engineering Measure
Type 2N1016B Silicon Alloy Transistor

QUARTERLY PROGRESS REPORT NO. 3
Covering period through March 31, 1963

Contract No. DA-36-039-SC-86743

Order No. 19065-PP-62-81-81

OBJECT OF STUDY

Improvement of production techniques to increase the reliability for high power silicon alloy transistors, especially Type 2N1016B.

PERSONNEL PREPARING REPORT

S. Chinowsky
T. Csakvari
E. G. Fatzer
J. R. Forys
R. W. France
E. Fowlkes
J. F. Henry
A. H. Long
D. L. Moore
T. G. Stehney
H. C. Ventura

TABLE OF CONTENTS

ABSTRACT

Progress on several phases of the process improvement program leading to completion in terms of revised process specifications is described. Continued development in other process improvement areas is described. Considerable data and preliminary analysis of the step-stress program results are given.

I. PURPOSE

The objective of the contract is the improvement of reliability of silicon alloy power transistors, particularly the Type 2N1016B, through the incorporation of various improvements in device fabrication. No changes in the basic device structure are planned. Rather, the planned improvements are aimed at increased device perfection through incorporation of new, more controllable processing techniques, redesign of some components of the encapsulation, and improved control of surface condition and stability. These modifications are expected to improve reliability by leading to more uniform device structures, current flow and heat flow, and to greater long-term chemical stability of the active element.

In support of the process improvement program, a reliability evaluation program utilizing high temperature storage step-stress testing is being undertaken. This program will be used to evaluate reliability of the transistors, before incorporation of any improvements, and after incorporation of all improvements. Individual improvements will be evaluated by test procedures aimed at the specific improvement under investigation.

II. PROCESS IMPROVEMENTS

A. Emitter Bridge Redesign - S. Chinowsky, D. Moore, R. France

Effort in this area had been limited in the past in view of a somewhat more basic approach concerning appraisal of techniques for investigating current distribution in the subject transistor. These studies have not provided sufficient information to date to warrant further restraint on the improvement of emitter bridge design.

Two approaches have been pursued to determine the effect of the emitter contact structure on the quality of the end product. The first of these provides for the use of a multiple contact emitter bridge as shown in Figure 1 (side view) and Figure 2 (top view). The primary significance of this design is that it will provide many current paths to the emitter junction and thereby reduce the "hot-spot" effect.

The second approach, a full contact system, as illustrated in Figure 3, includes a redesign of the "base-bridge" structure. Full area contacts are provided to the alloyed regions of the transistor. This system, although it may provide the ultimate in equallizing the emitter current distribution, contributes some undesirable features as well.

It has been necessary to modify the assembly procedure to obtain satisfactory attachment of the redesigned contacts. At present, the full-area contact system is definitely more difficult to use. Optimum etching and post-etch surface treatment (junction coating) may also be more difficult to perform. A complete evaluation of these factors will be made when a larger quantity of units have been fabricated and tested. These data will better define the problem areas associated with the redesign as well as the degree of reliability improvement.

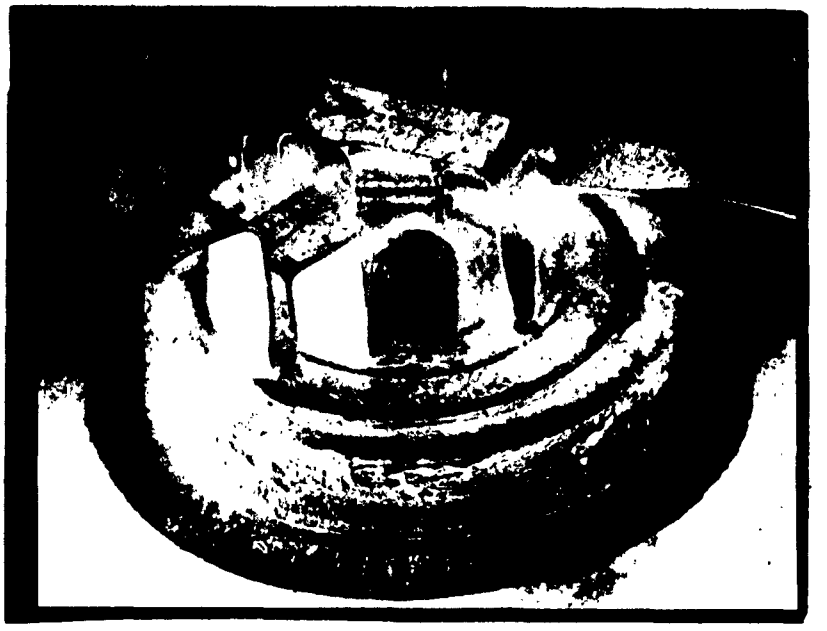

Figure 1. Model for study of multiple emitter bridge contact (side view)

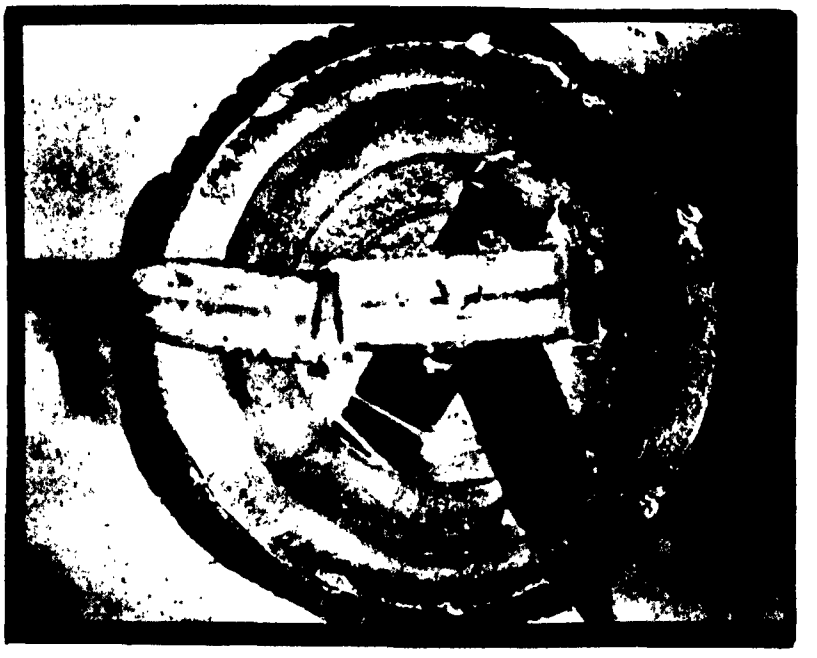

Figure 2. Model for study of multiple emitter bridge contact (top view)

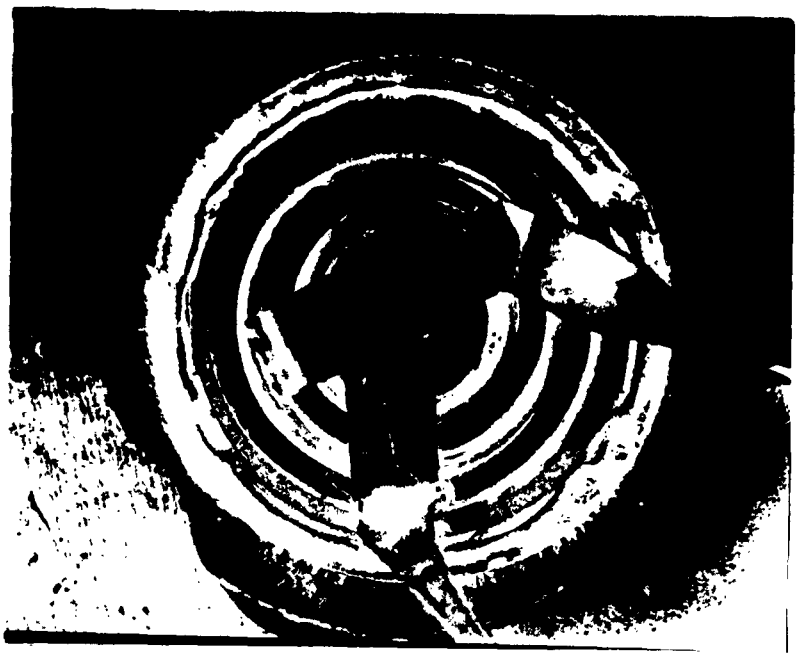

Figure 3. Model for study of full area contact system.

The full-area contact system offers one advantage which cannot be achieved by the other systems under investigation. It substantially reduces "leaching" or de-wetting of gold-silicon alloy from the base contact area at the surface of the unit. Figure 4 illustrates this condition.

There are more sophisticated approaches to the contact design which would substantially reduce the difficulties encountered during assembly. However, the impetus for investigations such approaches will depend on the results of the studies now in hand.

Figure 4. Top view of unit illustrating "leaching" of gold alloy.

Devices employing both of these contact systems have been fabricated. However, data available to date is inconclusive and will not be presented in this report.

Additional units are in the process of being fabricated and tested. All results will be given in the fourth quarterly report.

B. Weld Ring Redesign - D. Moore, R. France, B. Denis, C. Joyce

During the reporting period, the production order of seal rings was received from the vendor. These components showed further improvement over those previously received and are considered to be of satisfactory quality for production use.

To complete the evaluation of this component, a sizable number of assemblies were desired. To expedite fabrication of the group, they were assembled on the production line and one problem not previously in evidence was encountered. Misalignment of the cap and weld ring produced some final seal welds of low strength. This problem will be corrected through a minor modification of the weld ring (displacing the weld projection away from the outer ring edge of the seal ring, i.e. reducing the diameter of the weld projection) and improved locating fixtures during the welding operation.

Data was generated concerning weld joint strength of both old and redesigned seal rings. Samples were subjected to tensile test in two areas: pin seal (glass-to-metal emitter and base electrodes) and cap seal. Data on both pin weld seal and cap weld seal indicates a 30% increase in tensile strength. These data are briefly summarized in Table I. Figure 5 illustrates the tensile specimen used in this study.

	Pin Seal	Cap Seal
Old design (embossed projection)	450-700 lbs.	300-500 lbs.
New design (coined projection)	600-900 lbs.	400-700 lbs.

TABLE I. Tensile Strength Test Data

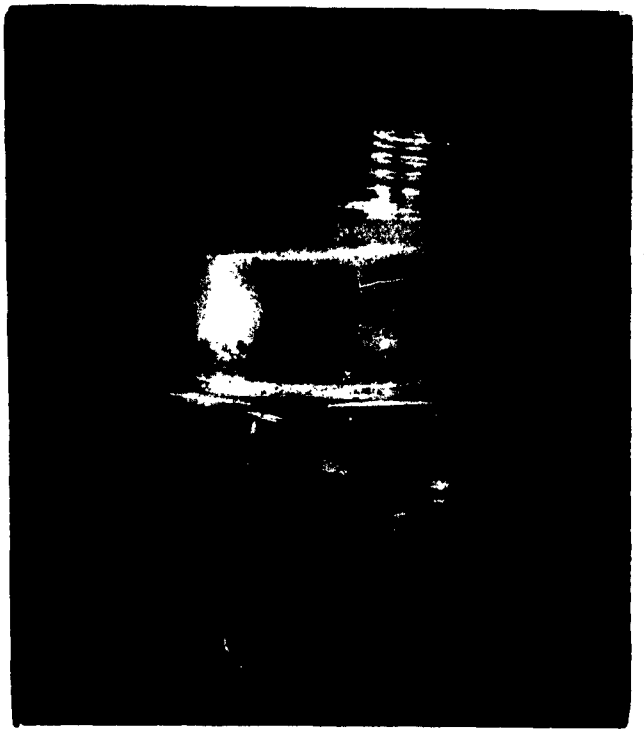

Figure 5. Sample used for tensile test of cap seal

The increase in strength was expected due to the geometry of the weld projection on the new design. Past reports have illustrated and discussed the relative merits of the coined projection and the embossed projection. Briefly, the coined projection provides two advantages: consistently uniform cross-section and improved back-up of projection by the seal ring material. In the area of the pin weld, the improved tensile strength characteristic can be attributed to back-up of the weld with a thicker section of material (seal ring), thus, minimizing deformation.

Additional evidence of improved weld joint strength was determined through centrifuge test. The device specification establishes a value of 5000 g's, minimum.

Present product employing the embossed seal ring exceeds this value, typically, by 50%. However, the new design employing the coined seal ring yields a typical value which exceeds the specification by 100%.

Leak test data has not yet been accumulated on a sufficient number of units to warrant a conclusion regarding the efficacy of the new seal ring design with respect to hermeticity. This will be completed in the next report period. It is expected from information previously reported on weld joint strength and the general quality of the weld as illustrated by cross-sections of joints, that a superior weld is achieved by all criteria.

C. Getters - J. Forys, J. Henry

The objective of this phase of work is to determine the efficacy of molecular sieves (getters) in the subject transistor for improved gain and I_{CEX} stability. A group of units incorporating tablet molecular sieves and another set of units with powdered molecular sieves were encapsulated, electrically tested, subjected to Group B environmental tests and again electrically tested. Results were compared to those obtained on a set of control units without moisture getters. A summary of observations and conclusions is as follows.

1. Post Encapsulation Test

There was little difference in yields between the control units and units with tablet molecular sieves following final testing after encapsulation. Units with powdered molecular sieves produced a somewhat higher yield than either of the other groups.

2. Electrical Test After Group B Environments

At this time, no conclusive relationship is apparent between I_{CEX} and the effect of moisture getters. There are indications that getters tend to stabilize or improve the leakage (I_{CEX}) characteristic of devices following a temperature environment (i.e. high temperature storage, temperature cycling, etc.). (Reference Table II).

The change in gain of units with moisture getters following environmental tests exhibited more stability than units not having moisture getters. This is especially evident after temperature cycling, operating life, and high temperature storage. Moisture getters appear to minimize the effect of temperature environments on gain stability. (Reference Table II).

No other significant parameter changes in units were evident following electrical tests after Group B environments.

A comparison of results obtained with the tablet molecular sieve versus the powdered molecular sieve indicated no obvious differences. The tablet sieve may, however, offer advantages in method of assembly in a device.

Plans are to conduct additional experimentation oriented towards conclusively establishing the effects of moisture getters as related to I_{CEX} and gain stability. It should be noted that the sample sizes available for data recorded in Table II were too small in number to determine significant differences. Future experiments will include sufficient number of units to establish conclusive results.

TABLE II

Average Parameter Changes of Devices With and Without Molecular Sieve After Group B Environmental Tests

ENVIRONMENT		Tablet Molecular Sieve Units			Powdered Molecular Sieve Units			Control Units		
		(1) ΔI_{CEX}	(1) ΔI_{EBO}	Δh_{FE}	(1) ΔI_{CEX}	(1) ΔI_{EBO}	Δh_{FE}	(1) ΔI_{CEX}	(1) ΔI_{EBO}	Δh_{FE}
1. Test Soldering, Temperature Cycling, Thermal Shock, Leak Test		-0.02	+0.05	+0.1	+0.1	-0.02	+0.06	+3.4	+0.1	+1.5
2. Shock, Centrifuge, Vibration Variable Frequency, Vibration Fatigue		+3.8	+1.3	-0.2	+4.7	0.0	-0.1	+0.3	+0.4	-0.04
3. Operating Life - 168 hours		-1.5	+1.9	+2.2	-0.04	+0.5	+1.5	-0.5	+0.1	+3.3
4. High Temperature Storage (168 hrs. at 150°C)	1 hr	+2.1	+0.6	+0.3	+0.6	+0.1	+0.04	+0.5	-0.3	+2.6
Test times following removal from 168-hr. storage.	5 hrs.	+1.7	+1.0	+0.5	+0.5	+0.2	+0.01	+0.8	-0.3	+2.7
	24 hrs.	+1.6	+1.2	+0.4	+0.7	+0.3	+0.1	+0.7	-0.3	+2.0
	28 hrs.	+1.6	+1.5	+0.4	+0.8	+0.3	+0.2	+1.0	-0.3	+2.5

(1) Milliamperes at 150°C

D. Base Material Modification - D. Moore, S. Chinowsky, R. France, B. Denis

Work on this phase of the contract was delayed pending receipt of the special chromium-cadmium-copper alloy components mentioned in the previous report. Delivery is promised in the near future.

Preliminary tests to compare thermal drops, junction-to-sink, of the standard tellurium copper alloy and the silicon-nickel-copper alloy indicate that for a given torque setting, the Te-Cu alloy is much superior. However, the application of higher torques, which the Si-Ni-Cu alloy will withstand, results in a more favorable comparison of Si-Ni-Cu with Te-Cu. Since the yield strength of the experimental alloy is several times that of the standard (Te-Cu) alloy, such a result is to be expected.

Since many factors are introduced when several materials are being compared, a revised evaluation program has been established for this phase of the program. Data which will be taken includes the following:

1. Torque vs. thread deformation.
2. Torque vs. device characteristic degradation.
3. Torque vs. thermal impedance, junction-to-sink.
4. Torque vs. thermal impedance, case-to-sink.

From this data, it is expected that a true comparative evaluation of the three materials can be made. This information, in conjunction with other considerations, will determine the final choice of a base material. Most of this information should be available for presentation in the next quarterly report.

E. Dry Air Environment - H. Ventura, J. Henry

The last report indicated that the design of the back end of the transistor line was 50% complete and it was expected to be finished by March 15. During this report period, the entire line was reviewed and a decision was made to build a completely new transistor line rather than re-build or modify the existing one. This decision has necessarily delayed action in accordance with the original plan. However, incorporating the process improvements into a line operation specifically designed to accept them is most advantageous in satisfying the reliability requirements of the contract. The design of the line is 85% complete. All of the long delivery items are now on hand. It is anticipated that installation will be done during the plant shutdown for vacation in early August. The convenience of scheduling such a major installation during that time is obvious.

F. Materials Preparation (Silicon) - S. Chinowsky, A. Knopp, J. Henry
T. Csakvari, B. Denis

1. Slice Etching

Evaluation of the alkali etch technique continued in this report period. Effort was directed at establishing some basic data regarding the etch rate on silicon, evaluation of slices for surface finish and flatness, alloying to alkali-etched surfaces and the influence of silicon so prepared on device characteristics.

Figure 6 displays a set of curves showing the rate of removal in the alkali etch vs. etch solution temperature. As is characteristic of most chemical reactions, the rate is very much temperature dependent. Note particularly the inflection point which occurs in each case. It is obvious from these data, which are both consistent and reproducible, that the alkali etch is amenable to good control when compared with the standard mixed acids etch technique.

Evaluation of wafers so etched for surface finish and flatness yielded encouraging information. Surface finish was shown to be reproducible as a function of time and temperature. Moreover, referring again to Figure 6, almost identical surface textures were observed at equivalent "removed thickness" levels regardless of the etch solution temperature. For example, points (1), (9), and (19) in Figure 6, yielded equivalent surface finishes. Thus, again, reproducibility is insured. Concerning flatness, wafers were evaluated for uniform removal across each face by recording thickness at the center and edge of each wafer prior to and after etch. Results are summarized in Table III.

T(°C) of Etch Solution	Thickness (mil) Before Etch		Thickness (mil) After Etch	
	Center	Edge	Center	Edge
50	10.25	10.25	9.70	9.72
70	10.25	10.25	9.25	9.25 to 9.50
90	10.25	10.25 to 10.30	9.00	8.95 to 8.98

TABLE III. Data of Removed Thickness Across Slices

The data indicates negligible "lensing" of wafers at 50°C. At the higher temperatures where etch rate will tend to vary even more, the data indicates little or no convexity. Again, it points out the desirability of the alkali-etch technique for the purpose of maintaining uniform slice thickness and, subsequently, uniform base width at the post-silicon wafer etch station.

Alloying to alkali-etched silicon was performed. Au-Sb preforms were alloyed under standard fusion conditions. The results indicate that the alloying mechanism shows no preference for any specific type surface as differentiated by the time-temperature conditions indicated at the numbered points on the curves in Figure 6. There does appear to be a tendency for more spreading of the alloy (transversely) when compared to the standard mixed acids etch. However, the difference is negligible in practice.

A number of transistors were fabricated on alkali-etched silicon wafers. The electrical test data indicates a very favorable comparison in terms of yield and voltage distribution with the control sample lot fabricated using the standard mixed acid solution.

In conclusion, the alkali-etch offers the following advantages over the standard mixed acids etch technique:

a. A readily controlled and reproducible technique for removal of damaged silicon from lapped wafers.

b. Suitable surface texture for alloying doped gold alloys.

c. Elimination of convexity of surfaces.

As a result of these studies, a process specification is being written to permit utilization of the alkali etch technique in production for the subject transistor. This portion of the product improvement work under the contract is, therefore, essentially complete.

2. Ingot Etching

After the experimental evaluation of the silicon ingot etch process, which indicated that the percent of rejected edge-cracked silicon slices has been decreased approximately to half, a process specification was prepared and approved. Checking the first 4,000 slices cut from etched silicon ingot, the percent of chipped and cracked silicon decreased to 4 to 5%.

Concurrent with the proposed investigation, Westinghouse initiated its own program designed to understand more thoroughly the parameters involved in the process of grinding the silicon ingot. During these experiments, the following parameters were investigated: grinding feed rate; cutting speed; cutting depth per pass; abrasive wheel.

As the result of these experiments the surface damaging effect of the grinding operation was substantially reduced at its source. Also, the percent of the chipped and edge-cracked silicon slices, prepared from silicon ingots ground by the revised grinding process, was reduced to the same level as the ground and etched silicon ingot slices. Therefore, the ingot etching phase of the contract work has become redundant and no further effort will be directed in this area.

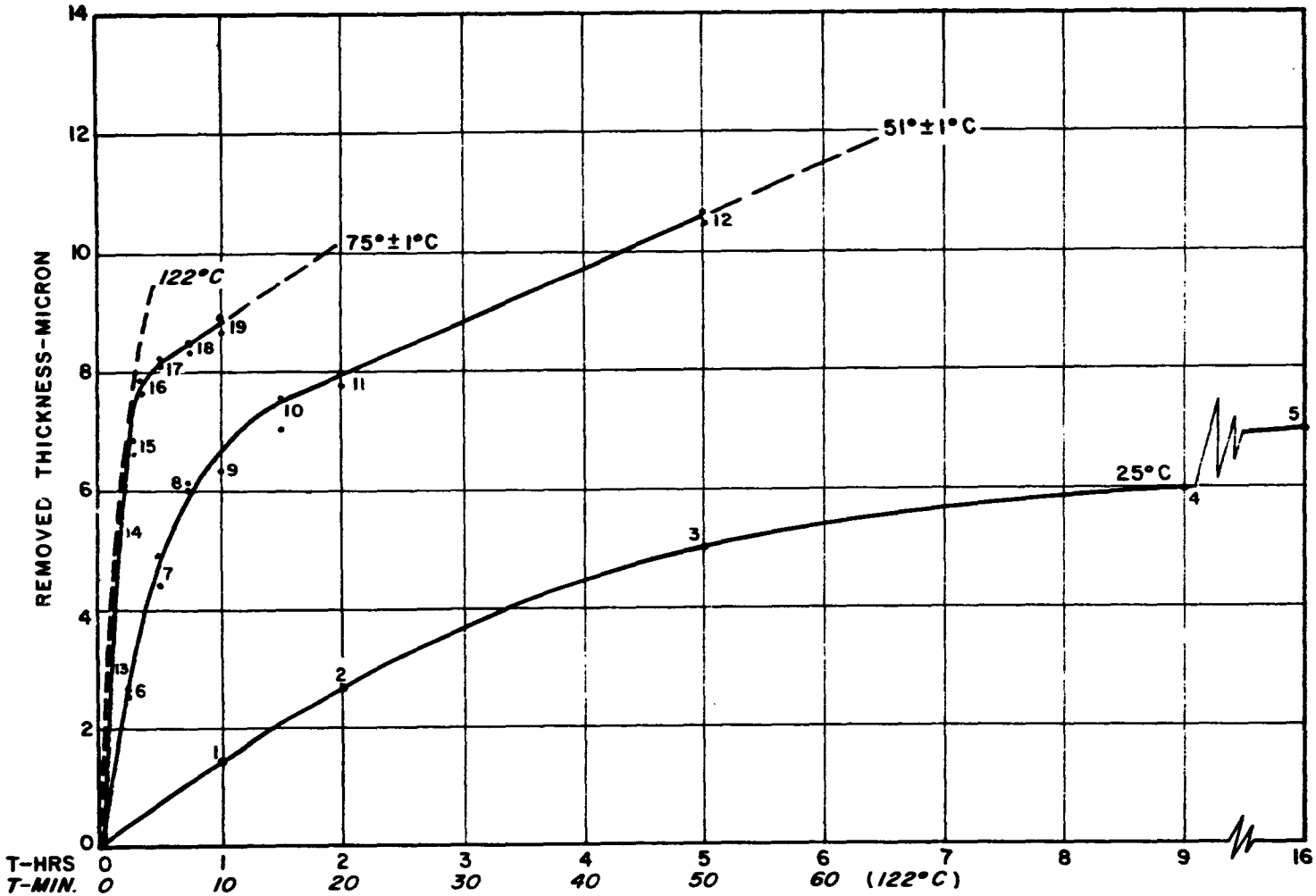

FIG. 6 REMOVED SILICON THICKNESS VS TIME OF KOH-ETCH

G. Material Preparation (Junction Alloys) - A. Long, J. Henry, J. Forys T. Stehney

The application of a beta-ray gauging system for dynamic non-contact thickness measurement of gold foil has been proposed. A system has been designed and evaluated for thickness measurement and control of "as-rolled" gold foils used in the production of alloy junctions and contacts to semiconductor materials.

The gauging system is an integral part of a cold rolling foil mill and monitors foil thickness, such that the rolling mill operator can control the thickness of the "as-rolled" gold foil by watching either a meter or a strip chart recorder. The ultimate intent is to optimize the thickness measurement to the highest possible level of accuracy consistent with the beta-ray gauging system and the application.

THEORY

The theory of a radio-active source emitting beta rays through a material of constant density, employed for thickness measurement, can be expressed by the universal absorption equation:

$$I = I_o e^{-\mu t} \qquad \text{(EQUATION I)}$$

Where:

I = measured source intensity
I_o = initial intensity of beta source
μ = mass absorption coefficient
t = material thickness

The mass absorption coefficient, μ, is proportional to the number of

electrons per unit volume of a material. The number of atoms, N, per cubic centimeter in a material of density, ρ, is:

$$N = \rho \frac{Na}{M} \qquad \text{(EQUATION II)}$$

M = molecular weight (grams/mole)

Na = avagadro's number (atoms/mole)

ρ = density (grams/cubic centimeter)

By multiplying equation II by the atomic number, Z (electrons/atom), the number of electrons per cubic centimeter, Ne, can be obtained:

$$Ne = \rho \frac{NaZ}{M} \qquad \text{(EQUATION III)}$$

It can be shown by equation III that a gram of any material contains about the same number of electrons, ie, that $\frac{MaZ}{M}$ is a constant. The density, ρ, is correlated to the mass absorption coefficient, μ, and more explicitly:

$$Me = \rho \frac{NaZ}{M} = \rho \text{ (constant)}$$

Thus it has been shown that the density of the measured material must be constant or its average deviation calculated as a segment of the accuracy tolerance of the gauging system.

The application of this theoretical equations can be applied to a physical system by considering the following concepts.

If an electrical potential is placed across two electrodes that are suspended a short distance apart in air, no current will flow since the air between the electrodes acts as an insulator. The two electrodes and the air between them form what is known as an ionization chamber.

If high speed electrons, such as beta particles, are allowed to enter this air, collisions with some of the air atoms will occur dividing the air molecules into equal and opposite charged ions. The ions are then attracted and collected on the electrode having a charge opposite to that of the ion. The migration of ions across the gas causes an electrical current to flow between the electrodes. Since the number of beta particles are small, the effective current developed in the ionization chamber is about 2×10^{-9} amps. However, currents of these levels can be measured very accurately with adequate electronic circuitry. Thus, the differences in current generated from radiation in the form of beta particles emitted from the source through various thicknesses of material of constant density and collected in the ionization chamber can be correlated to material thickness.

DISCUSSION:

The gauging system has a strontium-90 source which has a half-life of 25 years is collimated to measure an area 3/8" X 2" on the as-measured gold foil. The source centerline can be no less than 3/8" from the foil edge measurement.

The gauge throat can accommodate foil widths up to 5 inches. The limits of foil flutter passline, vertical motion of the foil within the gauge throat, were designed for a passline flutter of $\pm$ 0.008 inches.

The gauge has been designed to measure "as rolled" gold foil thickness ranging from 0.006 to 0.001 inches dynamically, sensitive to an average foil rolling speed of 280 inches per minute.

The gauge is further equipped with a fifteen range selector switch permitting the selection of fifteen separate thickness range options of $\pm$ 0.0001 to $\pm$ 0.001 inches full scale.

The gauge is calibrated by passing the collimated beta radiation from the source mount through various thickness of foil material where the thickness has been determined by a weight-geometry-density method.* The amount of radiation which passes through the gold foil thus reaching the detector or ionization chamber is measured as an electrical current and expressed as a percentage of the total collimated radiation emitted from the source and entering the ionization chamber. A curve results when the radiation intensity is plotted against the weight per unit area, i.e. thickness, of the gold foil. This curve is an approximation of an exponential function, but unlike a true exponential, falls to zero percent at a definite material thickness, i.e., is not asymptotic to the thickness axis.

The gauging system has been calibrated with an accuracy of $\pm$ 5.0%, where full scale sensitivity is set at 0.0002 inches, see Table I. The installation of this gauging system has resulted in improvement in the accuracy level of measurement from $\pm$ 0.00005 to $\pm$ 0.00001 inches. The result is an accuracy range of 20% of the accuracy range possible with former tooling or an improvement of 500%.

From Table I it is also noted that accuracy decreases and percent error increases with decreasing foil thickness range and full scale sensitivity.

Table II illustrates the data of thickness measurements made on various standard foil samples at four specific time intervals with a constant calibration curve. This indicator of the reliability of the gauging system results in a total maximum error of $\pm$ 1.5% at a full scale sensitivity of $\pm$ 0.0001 inches.

*A preform of known diameter is punched from the foil, and weighted on an analytical balance. From its weight, volume and density, its thickness can be accurately calculated.

To establish the range to range stability of the electronic circuitry of the gauging system, four gold foil standard samples 110C3A, 23D, 220D1A, and 220D1B of evaluated thickness of 1.019×10^{-3}, 1.040×10^{-3}, 1.585×10^{-3} and 1.665×10^{-3} inches, respectively, and illustrated as charts I, II, III, and IV were measured with all fifteen optional thickness ranges set for a given center scale thickness value and full-scale sensitivity. The two samples in the 1.10×10^{-3} inch thickness category had maximum percentage error of -2%, $\pm$ 1% at a full scale sensitivity of 0.00002 inches (see charts I and II). The two samples illustrated as charts III and IV had errors of $\pm$ 1.0% at full scale sensitivities of 0.5×10^{-3} inches.

As well as significant improvements in measurement and control of gold foils, the beta gauging system offers non-contact (contamination-free) continuous measurement of gold foils, dynamically, during their fabrication. With the previous system of thickness measurement and control, only intermittent local "spot checking" of the gold foil was possible.

CONCLUSION:

The application of a beta gauging system has been designed and evaluated for thickness measurement and control of "as-rolled" gold foil for semiconductor device manufacture. The system has a calibrated accuracy 10 x 10^{-6} inches or $\pm$ 5% of full scale sensitivity of 2×10^{-4} inches for gold foils 0.001 inches in thickness. The reliability of the gauging system and the range to range stability were found to be approximately $\pm$ 2% or $\pm$ 4×10^{-6} inches.

The adoption of this gauging system has accomplished continuous, non-contact, and dynamic "as-rolled" gold foil thickness measurement and control with a 500% improvement in accuracy of measurement.

- TABLE 1 -

SUMMARY OF BETA GAUGE CALIBRATION DATA

SAMPLE NO.	CALCULATED THICKNESS (0.001 INCH)	FULL-SCALE SENSITIVITY (0.001 INCH)	RANGE NO.	MEASURED THICKNESS (0.001 INCH)	PERCENT ERROR
708D2	5.22	± 1.00	15	5.21	-0.5%
113E2	5.10	± 1.00	15	5.08	-1.0%
708C2	4.74	± 1.00	15	4.75	+0.5%
220D1B	4.15	± 1.00	14	4.14	-0.5%
110D8B	3.03	± 0.50	13	3.05	+2.0%
706M2	2.77	± 0.50	13	2.76	-1.0%
		± 0.50	12	2.76	-1.0%
110D3A	2.374	± 0.50	12	2.365	-0.9%
220D1B	1.658	± 0.25	10	1.665	+1.4%
		± 0.25	9	1.665	+1.4%
		± 0.25	8	1.655	-0.6%
220D1A	1.601	± 0.25	10	1.585	-3.2%
		± 0.25	9	1.585	-3.2%
		± 0.25	8	1.585	-3.2%
706D2A	1.351	± 0.25	8	1.335	-3.2%
		± 0.25	7	1.337	-2.8%
		± 0.25	6	1.335	-3.2%
		± 0.10	4	1.343	-4.0%
		± 0.10	3	1.341	-5.0%
219F2A	1.198	± 0.25	6	1.205	+1.4%
		± 0.10	2	1.203	+5.0%
23D	1.045	± 0.10	1	1.040	-5.0%

- TABLE II -

RELIABILITY INDICATION OF BETA GAUGING SYSTEM

SAMPLE NO.	CALC. THICKNESS (MILS)	FULL-SCALE SENSITIVITY (MILS)	RANGE NO.	MEASURED THICKNESS (MILS) (A)	(B)	(C)	(D)	PER CENT ERROR
110C3A	1.0455	± 0.10	1	1.018	1.018	1.017	1.020	± 0.75%
		± 0.25	6	1.010	1.010	1.010	1.010	± 0.0 %
23D	1.0450	± 0.10	1	1.044	1.044	1.042	1.040	± 1.0 %
		± 0.25	6	1.040	1.040	1.035	1.035	± 0.5 %
219F2	1.200	± 0.10	2	1.201	1.204	1.200	1.203	± 1.0 %
		± 0.10	3	---	1.208	1.202	1.203	± 1.5 %
		± 0.25	6	1.202	1.209	1.202	1.205	± 0.7 %
		± 0.25	7	1.195	1.202	1.198	1.195	± 0.7 %
706D2A	1.351	± 0.10	3	1.338	1.340	1.338	1.338	± 0.5 %
		± 0.10	4	1.342	1.346	1.342	1.343	± 1.0 %
		± 0.25	6	1.330	1.335	1.335	1.335	± 0.5 %
		± 0.25	7	1.335	1.340	1.337	1.337	± 0.5 %
		± 0.25	8	1.335	1.340	1.335	1.335	± 0.5 %
220D1A	1.6017	± 0.25	7	1.575	1.580	1.575	1.580	± 0.5 %
		± 0.25	8	1.580	1.585	1.585	1.585	± 0.5 %
		± 0.25	9	1.585	1.590	1.585	1.585	± 0.5 %
		± 0.25	10	1.580	1.585	1.580	1.585	± 0.5 %
220D1B	1.658	± 0.25	7	1.645	1.645	1.645	1.645	± 0.0 %
		± 0.25	8	1.655	1.655	1.655	1.655	± 0.0 %
		± 0.25	9	1.665	1.665	1.665	1.665	± 0.0 %
		± 0.25	10	1.665	1.670	1.665	1.665	± 0.5 %
110D3A	2.374	± 0.50	12	2.365	2.370	2.365	2.365	± 0.2 %

- TABLE II -

RELIABILITY INDICATION OF BETA GAUGING SYSTEM

SAMPLE NO.	CALC. THICKNESS (MILS)	FULL-SCALE SENSITIVITY (MILS)	RANGE NO.	(A)	(B)	(C)	(D)	PER CENT ERROR
706M2	2.770	± 0.50	12	2.760	2.760	2.760	2.760	± 0.0 %
		± 0.50	13	2.760	2.760	2.760	2.755	± 0.2 %
220D1B	4.15	± 1.00	14	---	4.14	4.14	4.14	± 0.0 %
113E2	5.10	± 1.00	15	---	5.08	5.08	5.08	± 0.0%

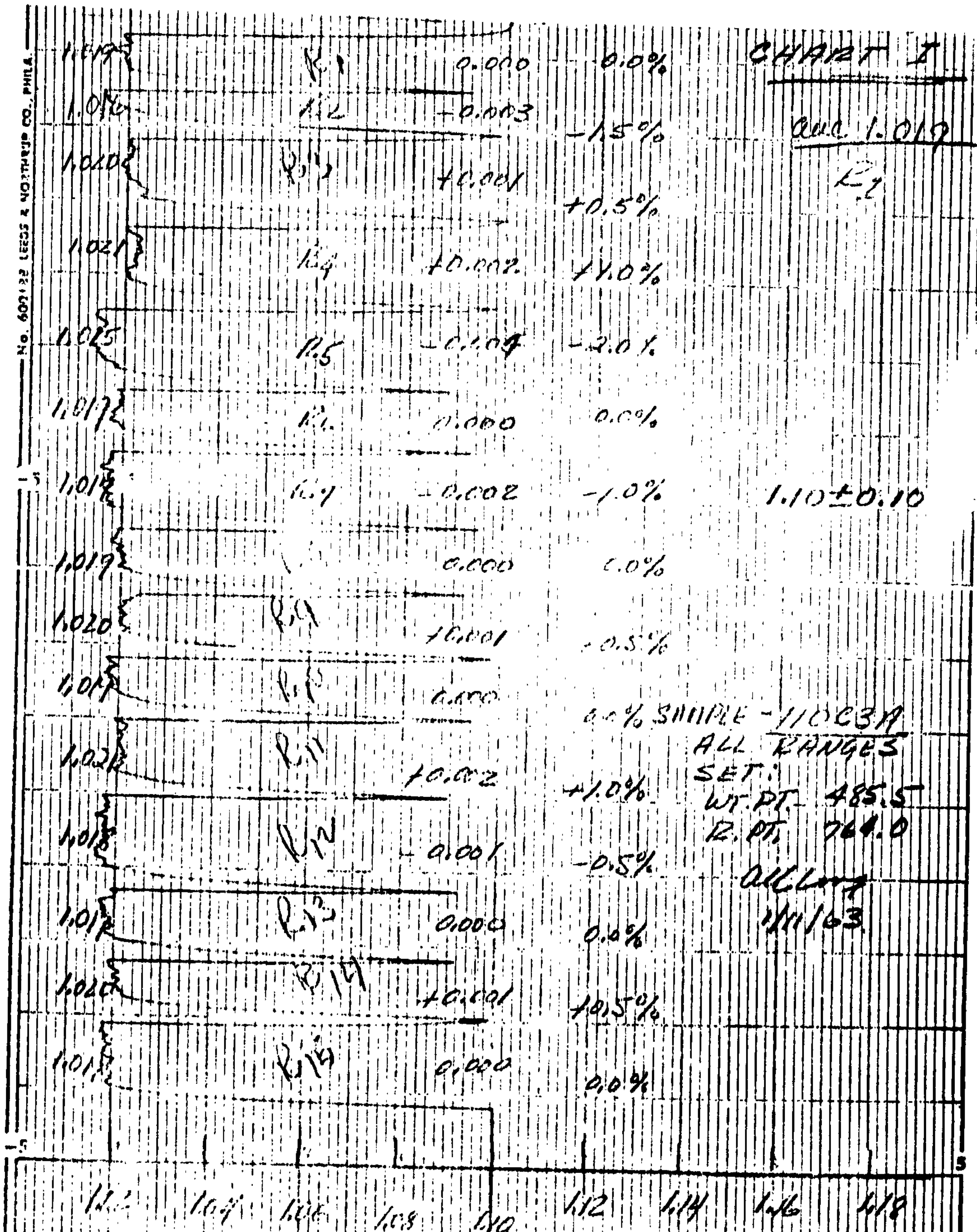
No. 60?122 LEEDS & NORTHRUP CO., PHILA.
CHART I
1.10±0.10
SAMPLE - 110C3A
ALL RANGES
SET:
WT. PT. 485.5
R. PT.
0.000 0.0%
-0.003 -1.5%
+0.001 +0.5%
+0.002 +1.0%
-2.0%
-0.002 -1.0%
+0.002 +1.0%
-0.001 -0.5%
+0.001 +0.5%
1.12
1.14
1.16
1.18

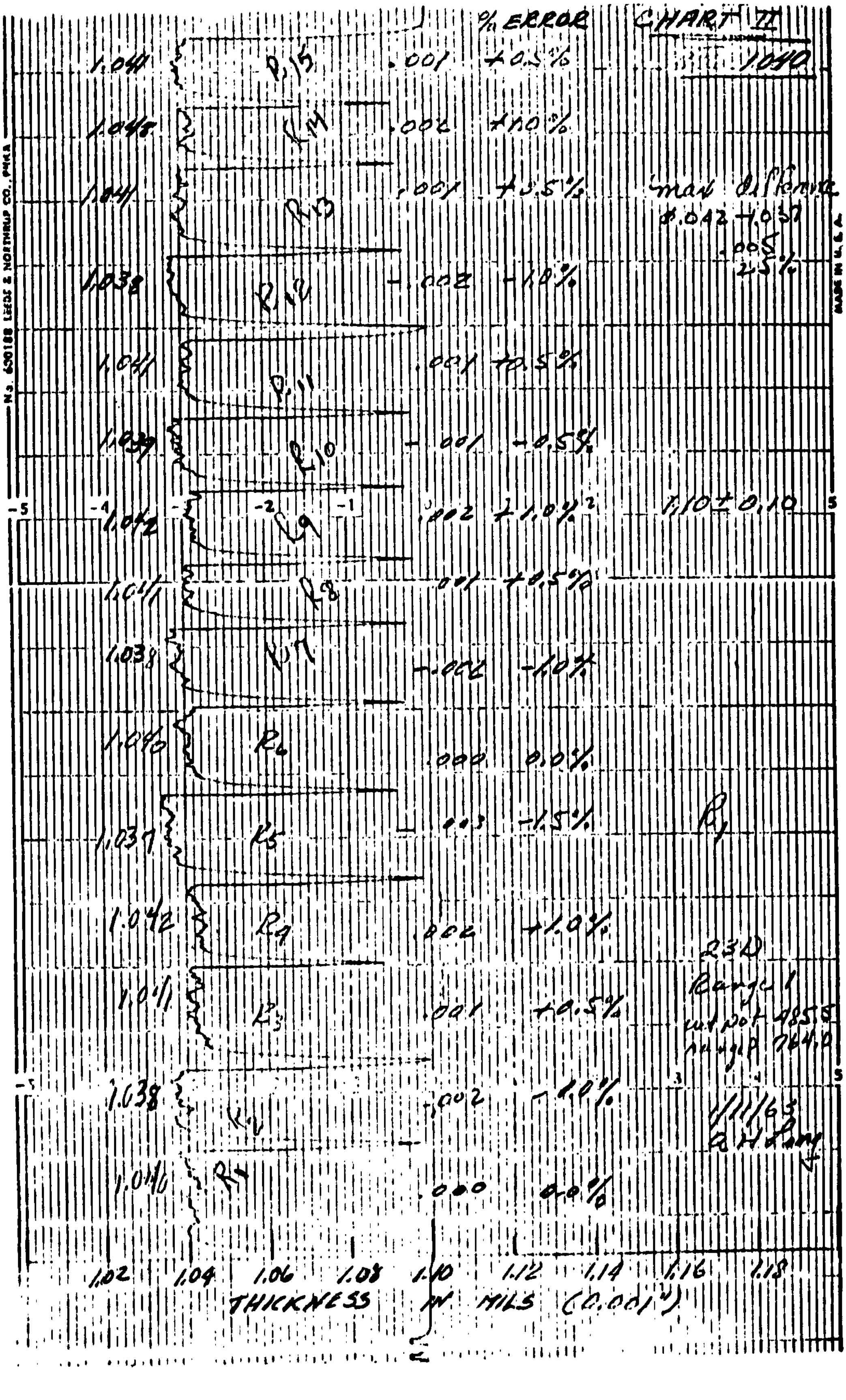
% ERROR
CHART II
1.040
1.041 R15 .001 +0.5%
1.042 R14 .002 +1.0%
1.041 R13 .001 +0.5%
max difference
.042 - .037
.005
2.5%
1.038 R12 -.002 -1.0%
1.041 R11 .001 +0.5%
1.039 R10 -.001 -0.5%
1.042 R9 .002 +1.0%
1.10 ± 0.10
1.041 R8 .001 +0.5%
1.038 R7 -.002 -1.0%
1.040 R6 .000 0.0%
1.037 R5 .003 -1.5%
R1
1.042 R4 .002 +1.0%
1.041 R3 .001 +0.5%
1.038 R2 .002 -1.0%
1.040 R1 .000 0.0%
1.02 1.04 1.06 1.08 1.10 1.12 1.14 1.16 1.18
THICKNESS IN MILS (0.001")

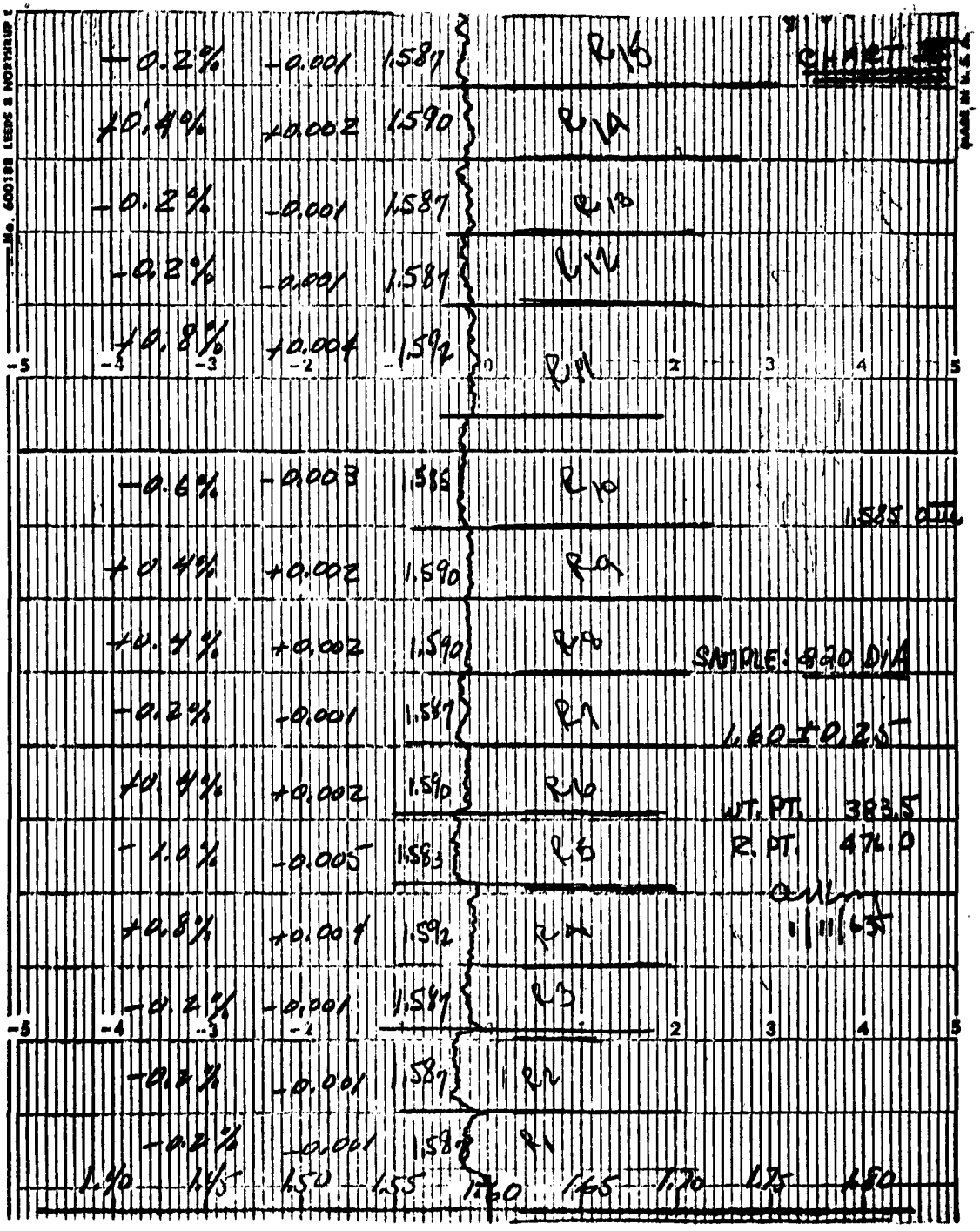
CHART
SAMPLE: 820 DIA
1.60 ± 0.25
WT. PT. 383.5
R. PT. 474.0
1.585 OIL
-0.2%
+0.4%
-0.2%
-0.2%
+0.8%
-0.6%
+0.4%
+0.4%
-0.2%
+0.4%
-1.0%
+2.8%
-0.2%
-0.2%
-0.2%
R16
R14
R13
R12
R11
R10
R9
R8
R7
R6
R5
R4
R3
R2
R1
1.587
1.590
1.587
1.587
1.592
1.586
1.590
1.590
1.587
1.590
1.583
1.592
1.587
1.587
1.587
1.590
1.50
1.55
1.60
1.65
1.70
1.75
1.80

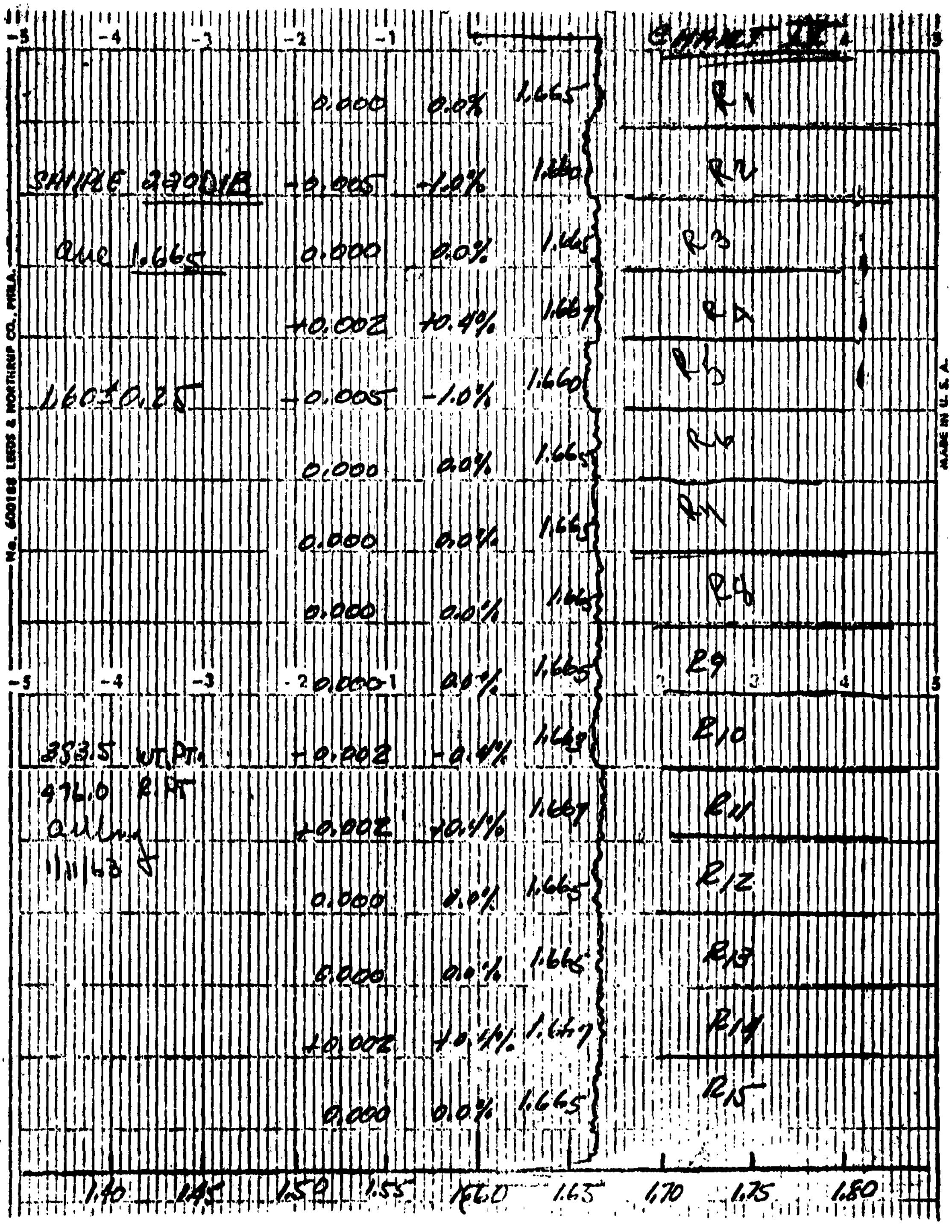
R1
R2
R3
R4
R5
R6
R7
R8
R9
R10
R11
R12
R13
R14
R15
0.000 0.0% 1.665
-0.005 -1.0% 1.660
0.000 0.0% 1.665
+0.002 +0.4% 1.667
-0.005 -1.0% 1.660
0.000 0.0% 1.665
0.000 0.0% 1.665
0.000 0.0% 1.665
0.000 0.0% 1.665
+0.002 +0.4% 1.667
+0.002 +0.4% 1.667
0.000 0.0% 1.665
0.000 0.0% 1.665
+0.002 +0.4% 1.667
0.000 0.0% 1.665
AVG 1.665
283.5 WT PT
1.40
1.45
1.50
1.55
1.60
1.65
1.70
1.75
1.80
MADE IN U. S. A.

H. Material Preparation (Gold-Plated Molybdenum) - E. Fatzur, R. France
J. Henry, J. Forys

The last quarterly report summarized the process information regarding the dual approach of rack plating using the gold strike-diffuse-gold plate-diffuse technique and barrel plating using Korbelak's system of chromium strike-nickel strike-gold plate. Samples fabricated by both techniques have proven to be satisfactory in that they satisfy both the acid dip test and the "use" test. In the former, plated molybdenum samples are dipped in a mixed acid solution. Acceptance as "good" product is based on the ability of the plating to prevent the attack of the acid solution on the substrate molybdenum. This indicates that the plated layer of gold is both continuous (no "pin holes") and adherent. The "use" test consists of brazing plated molybdenum to a copper base and subsequent rupture of the brazed joint by physically dislodging it from the base. Examination of the exposed brazed joint yields information regarding the quality of the metallurgical bond. In practice, the joint is examined for voids and degree of adherence of the molybdenum.

Since either technique described above has been proven to yield quality product, the choice of one or the other can be made on the basis of available equipment, manufacturing cost, etc. Equipment is on hand to pursue the rack plating technique. It is not available, on a production basis, for barrel plating. Therefore, in terms of the contract commitment, the rack plating technique will be introduced as the final solution. Work may continue on the alternate technique if there is reason to believe that a cost advantage can be achieved.

A process specification has been written and the rack plating technique is in limited production on some devices.

J. Fusion Assembly - R. Nandor, J. Henry

Experimental runs using a mechanical fixture in place of the present hand alignment method were made and evaluated. A fair degree of success was achieved; however, the station yield was 66% as compared to 90% for the hand assembled devices. Several difficulties and advantages were encountered.

1. The basic gold preforms are slightly bowed and exhibit a small degree of burring after punching which make it difficult to nest the assembly in the alignment die which is machined for very close tolerances.

2. The mechanical alignment method is less fatiguing to the operator.

3. Alignment of preforms and silicon were, on the average, better than hand alignment prior to alloying; however, results at post alloying gave relatively low physical yield. This problem is attributed, again, to the lack of very flat preforms.

4. With experience, the fixture can produce a lower labor cost for this operation.

Thus, to master this technique, it will be necessary to improve the flatness of the gold preform and eliminate burrs generated in preform punching. More experience by the operator is also needed before the technique can compete operational-wise with hand alignment. Work in this area will continue through the next report period.

K. Hard Solder Assembly - R. France, T. Csakvari, J. Forys

Two approaches were taken to improve the brazed joints of the transistor structure and thereby insure a full area contact between the basic device and the encapsulation base.

1. Optimize the present process by minimizing or eliminating the voids between the molybdenum disc and encapsulation base.

2. Investigate new materials or methods of making the hard solder joint.

Significant improvement of the present process has been established and modifications so made have been running successfully in production for some time. The method used is pre-tinning of the gold plated molybdenum disc with a vacuum tube grade of BT braze alloy in a separate furnace operation prior to joining it to the copper base and seal ring. Coupled with operation inspection by Quality Control and simplified use tests of the materials going into the operation, process control is established on both materials and manufacture. Use tests established are as follows:

a. Physical testing of a sample from each rack of gold plated molybdenum to establish the plating quality and braze wetting properties.

b. Physical inspection of each lot of nickel plated seal rings.

c. Destructive testing of sample lots of brazed assemblies throughout production runs.

d. Establish parts "bank" for monitoring processes per se.

The above-mentioned is established in process specifications.

Further analysis of the final electrical test parameters taken by Quality Assurance for production lot acceptance indicates that only three devices from lots representing fifty thousand units failed to meet the thermal impedance specification of 0.7°C/watt. Destructive analysis of present thermal impedance rejects indicates that the base assembly can be reliably omitted as a factor leading to device failure for thermal conductivity parameters.

Establishment of ultrasonic pulse echo techniques, as an additional flaw detection method on this operation, has not been established for production use. The equipment has been transferred to the Quality Assurance Laboratory for further work.

Probable application of new materials for performing the base braze have primarily been centered on the substitution of new braze materials and powdered molybdenum. These developments have progressed significantly and devices have been fabricated for evaluation. The objective has been to generate materials that are prepared in-house where control of quality (and cost) can be more closely scrutinized. Metallurgical bonding of molybdenum and soldering materials is difficult due to the difference in surface-free energies of the materials. Therefore, a new braze material (silicon, copper, nickel and silver) was investigated as a substitute for gold plating and/or BT solder.

To investigate the improvement of the hard soldered joint between molybdenum and copper, the following groups of molybdenum discs were precoated with a silver-copper-nickel-silicon alloy: unlapped and unplated sheet molybdenum discs; gold-plated powdered molybdenum discs; and unplated powdered molybdenum discs.

The finished devices were tested and evaluated. Group A and Group C have been failed on electrical evaluation. Upon cross-sectioning, the failed units, it was found that the silicon wafer cracked usually where the bridge is attached to the silicon. Since it was necessary to precoat the top of the molybdenum discs with a silver alloy (otherwise the fusion does not wet the unplated molybdenum contact), the cracking was probably due to the different thermal expansion of the silver alloy and the silicon. (See Figure 7). Group B units passed electrical evaluation but were marginal on thermal drop test. Cross-sectioning indicated excess voids in the joint between the copper base and molybdenum disc. Since previous experiments always yielded sound joints (see Figure 8) between the two components, experiments have been initiated to find the answer to this problem.

Though a suitable process improvement has been attained by application of the pre-tinning technique, effort will continue on the second approach discussed above. The potential advantages of the latter approach in terms of quality control of materials and fabrication processes as well as lower cost, warrant this action.

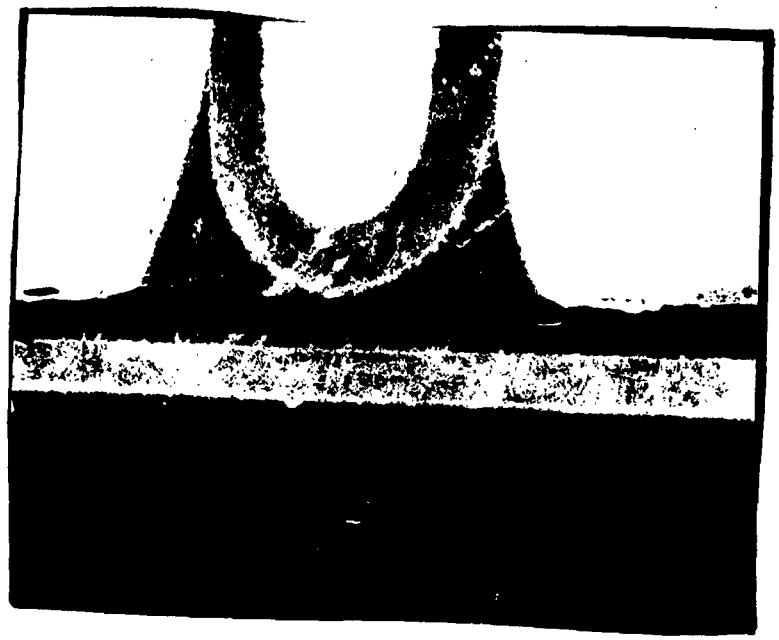

Figure 7. Cross-section illustrating cracked silicon under bridge contact.

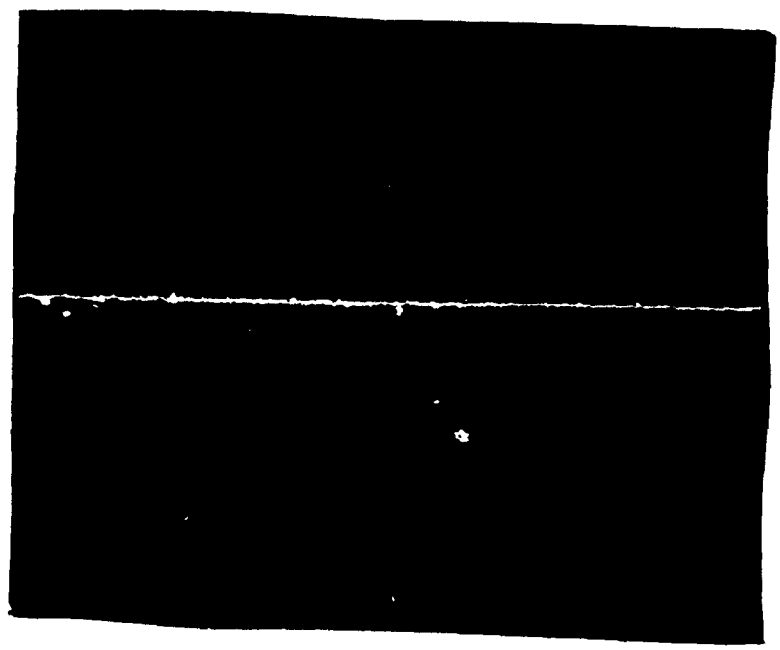

Figure 8. Cross-section of void-free braze joint

L. Investigation of Surface Passivation Coatings - T. Stehney

It has been noted in past reports that the present process for surface passivation of the subject transistor is characterized by the high voltage and low leakage junctions. This process was originally developed as a result of experience in the alloyed high power rectifiers and transistors. It uses an organic resin as the surface coating.

In the past few years, planar transistors have come into existence. In the process of fabricating planar transistors, oxide layers over the junctions for surface passivation are generated as a natural consequence of the diffusion process. It was also found that this oxide layer protects the surface from the atmosphere and maintains the surface states such that the device characteristics are significantly more stable than other prevailing technology could offer. The use of oxide passivation became wide spread in the industry. However, the planar technology has been applied, and still is, primarily for higher frequency devices and low power operation. Especially fortunate is that the collector junction voltage usually operates in the range of 60 to 100 volts or less. The improvement of junction characteristics have been very significant.

For higher voltage junctions, little or no experience could be drawn on to indicate that oxide passivation can be depended on. Recently, however, the situation has been gradually clearing up. Most manufacturers, after much experimentation, have reached the present state of art limit of about 200 volts. Further improvement has been rather impractical at this point in time. On the other hand, the organic resin has proven itself to be extremely suitable for high voltage junctions. Almost all high voltage device junctions in the industry are now coated with organic resins. It has been reported that single junctions well over 3000 volts at about 150°C have been successfully processed with organic coatings.

Based on the latest industrial knowledge concerning the technology of the high voltage junction termination, it is certain that the present process employed for the subject device is entirely adequate. This is also confirmed by the step stress evaluation results. Referring to the graphs of Figures 6 to 8 in Section III, the 50 percentile readings are well within data limits even after extensive storage of 3000 hours at 300°C.

In view of these test results, it is now obvious that no basic process change is required. However, the line control of the process from junction etching through encapsulation must be tightened to reduce the spread of the junction leakage current distribution within a production lot. This portion of work should therefore be consolidated with the control of the encapsulation line as reported under Section II-E.

III. RELIABILITY MEASUREMENT - STEP STRESS PROGRAM

Preliminary Data Analysis - E. Fowlkes, J. Forys

A summary of the failures obtained to date on the program outlined in the first quarterly report are presented in Tables I and II for the constant temperature and constant time experiments respectively. The anomaly reported earlier in the data of Table I, in that fewer failures occurred at 300°C than at 250°C for times longer than 168 hours, was investigated with no logical explanation resulting. However, investigation has revealed that a change in power test equipment circuitry was made around the 1000 hour test point of experiment IA and this tended to have some inflationary effect on the total number of failures observed. The power test circuitry problem was corrected and it was found that the failures which had occurred were actually good on retest. As a result the number of failures in Tables I and II has been adjusted for all stress levels (temperatures) where the inflationary effect of power test was verified.

A. Parameter Vs. Time - 5th, 50th, 95th Percentiles (V_{BE}, Gain, I_{CEX})

For the constant temperature experiments, graphs of parameters of interest versus time at temperature were plotted for the 5th, 50th, and 95th percentiles (Ref: Figures 1 to 8). These graphs indicate the parameter degradation over time.

Figures 1 and 2 (V_{BE} vs. time) exhibit the unusual condition where, at 200°C and after 2000 hours storage time, 50 percent of the units were found out of specification whereas this situation was not evident at the higher temperatures of 250°C and 300°C for an equivalent storage time. This anomaly was investigated but an explanation cannot be offered at this time.

Figure 3 (Gain vs. Time) shows that at 150°C units tend to initially in-

crease in gain, level off and remain fairly stable out to 3000 hours storage time. At 200°C, 250°C and 300°C storage temperatures an initial increase in gain is apparent with a subsequent degradation effect with storage time. An overall comparison of figures 3-5 displays the condition of increasing gain degradation with increased temperature stress.

I_{CEX} vs. time is shown in figures 6-8. An overall comparison indicates an increasing degradation effect with elevated temperatures as was apparent with the gain parameter. At 150°C storage, I_{CEX} has shown good stability out to 3000 hours.

B. Linear and Transformed Parameter Vs. Linear and Transformed Time - 50th Percentile (V_{BE}, I_{CEX}, Gain)

For the constant temperature experiments, graphs of linear and transformed parameters of interest versus linear and transformed time at temperature were plotted for the 50th percentiles. All temperatures for a parameter are included on the same graph. Figures 9 to 23 present the following transformations for V_{BE}, I_{CEX} and Gain: linear parameter vs. linear time, linear parameter vs. log time, log parameter vs. linear time, $\frac{\text{parameter reading } (t_x)}{\text{parameter reading } (t_o)}$ vs. linear time, $\frac{\text{parameter reading } (t_x)}{\text{parameter reading } (t_o)}$ vs. log time.

Figures 9 to 13 display the anomaly of the 200°C effect on V_{BE} as already exhibited by figure 1 and also an unusual situation which occurred at 300°C. The graphs illustrate that 300°C storage out to 3000 hours has had no more adverse effect on V_{BE} than did the 150°C storage temperature.

Figures 14 to 18 indicate that the effect on I_{CEX} is related to the level of stress as the value of I_{CEX} approaches the specification limit with

increase [illegible]ure. After 3000 hours storage at temperatures as high as 300°C, 50 percent of the units still remain within the specification [illegible] 350°C, however, 50 percent of the units failed to meet the limit after approximately 500 hours storage.

Figures 19 to 23 show, as was the case with I_{CEX}, that the effect on gain is related to the level of stress since the value of gain approaches the specification limit with increased temperature. In each of the stress temperatures with the exception of 350°C, initial effect on gain was to increase in value with subsequent degradation with storage time out to 3000 hours. At 350°C the effect on gain was immediate in that 50 percent of the units was less than the specification limit after 48 hours of storage time.

Transformations were selected which were thought to have the greatest chance of linearizing the V_{BE}, I_{CEX}, and Gain data. At this time it appears that none of the transformations selected are satisfactory for linearizing the data.

C. Cumulative Percent Failures Vs. Log Time

A plot of cumulative percent failures vs. log time for the constant temperature experiments is shown in figure 24 with all temperatures presented on the same graph. The anomaly in that fewer failures occurred at 300°C then at 250°C for times longer than 168 hours is quite apparent. It is, likewise, unusual that after 2000 hours more failures occurred at 200°C then at 250°C. Performance of devices at 150°C has been such that two failures have occurred after 3000 hours.

D. Temperature (10^3/°K) Vs. Cumulative Percent Failures

For the constant time experiments figure 25 is a plot of the cumulative

failure distribution in temperature (plotted $10^3/°K$) for 168-hour, 336-hour, 500-hour, 672-hour, and 1000-hour time intervals. The data were not corrected for the effects of the previous stress levels. The 1000-hour time interval as indicated by the graph has produced somewhat unexpected results in that fewer failures have occurred than at the 672-hour time interval. Of particular interest is the apparent inflection on all curves at the (approx.) 250°C level. This indicates that a new failure mode may be manifesting itself.

E. Temperature ($10^3/°K$) Vs. Log Time - 50th Percentiles of the Failure Distributions

Figure 26 is a plot of temperature ($10^3/°K$) vs. log time using the 50th percentile points of the failure distributions for both the constant temperature and constant time experiments. With the exception of the abnormal 300°C point indicating that 50 percent of the units fail after 1400 hours, the remaining points enable one to approximate a line. From this line, an estimate of time to failure for 50 percent of the units at a given storage temperature may be obtained. Figure 26 shows, in effect, time to failure as a function of temperature.

F. Conclusions

From the data generated to date, and with particular reference to Figure 25 which plots temperature ($10^3/°K$) vs. cumulative percent failures, it appears that the final specification for the improved 2N1016 should include storage temperature stress level(s) below 250°C in order to avoid the introduction of the second failure mode.

failure distribution in temperature (plotted $10^3/°K$) for 168-hour, 336-hour, 500-hour, 672-hour, and 1000-hour time intervals. The data were not corrected for the effects of the previous stress levels. The 1000-hour time interval as indicated by the graph has produced somewhat unexpected results in that fewer failures have occurred than at the 672-hour time interval. Of particular interest is the apparent inflection on all curves at the (approx.) 250°C level. This indicates that a new failure mode may be manifesting itself.

E. Temperature ($10^3/°K$) Vs. Log Time - 50th Percentiles of the Failure Distributions

Figure 26 is a plot of temperature ($10^3/°K$) vs. log time using the 50th percentile points of the failure distributions for both the constant temperature and constant time experiments. With the exception of the abnormal 300°C point indicating that 50 percent of the units fail after 1400 hours, the remaining points enable one to approximate a line. From this line, an estimate of time to failure for 50 percent of the units at a given storage temperature may be obtained. Figure 26 shows, in effect, time to failure as a function of temperature.

F. Conclusions

From the data generated to date, and with particular reference to Figure 25 which plots temperature ($10^3/°K$) vs. cumulative percent failures, it appears that the final specification for the improved 2N1016 should include storage temperature stress level(s) below 250°C in order to avoid the introduction of the second failure mode.

TABLE I

Step Stress Program - Experiment IA

Cumulative Number Of Failures In High Temperature Storage

Parameter Degradation Section

Temperature Factor Held Constant

	TEMPERATURE				
Time In Hours	150°C	200°C	250°C	300°C	350°C
2	-	-	-	-	30
4	-	-	-	-	45
8	-	-	-	-	48
16	-	-	-	-	48
48	0	0	2	8	50
168	0	0	17	13	
312	1	0	32	15	
500	1	0	33	18	
1000	1	4	34	21	
1500	1	23	37	27	
2000	1	40	37	28	
2500	2	45	38	29	
3000	2	47	39	30	

TABLE II

Step Stress Program - Experiment IB

Cumulative Number Of Failures In High Temperature Storage

Catastrophic Failure Section

Time Factor Held Constant

TIME IN HOURS

Temperature (°C)	168	336	500	672	1000
150	0	0	0	1	0
175	1	0	0	2	1
200	3	4	11	15	12
225	8	27	35	45	34
250	21	40	46	49	
275	36	41	47	49	
300	45	44	48		
325	49	49	49		
350	49	50			

V_{BE} vs Time

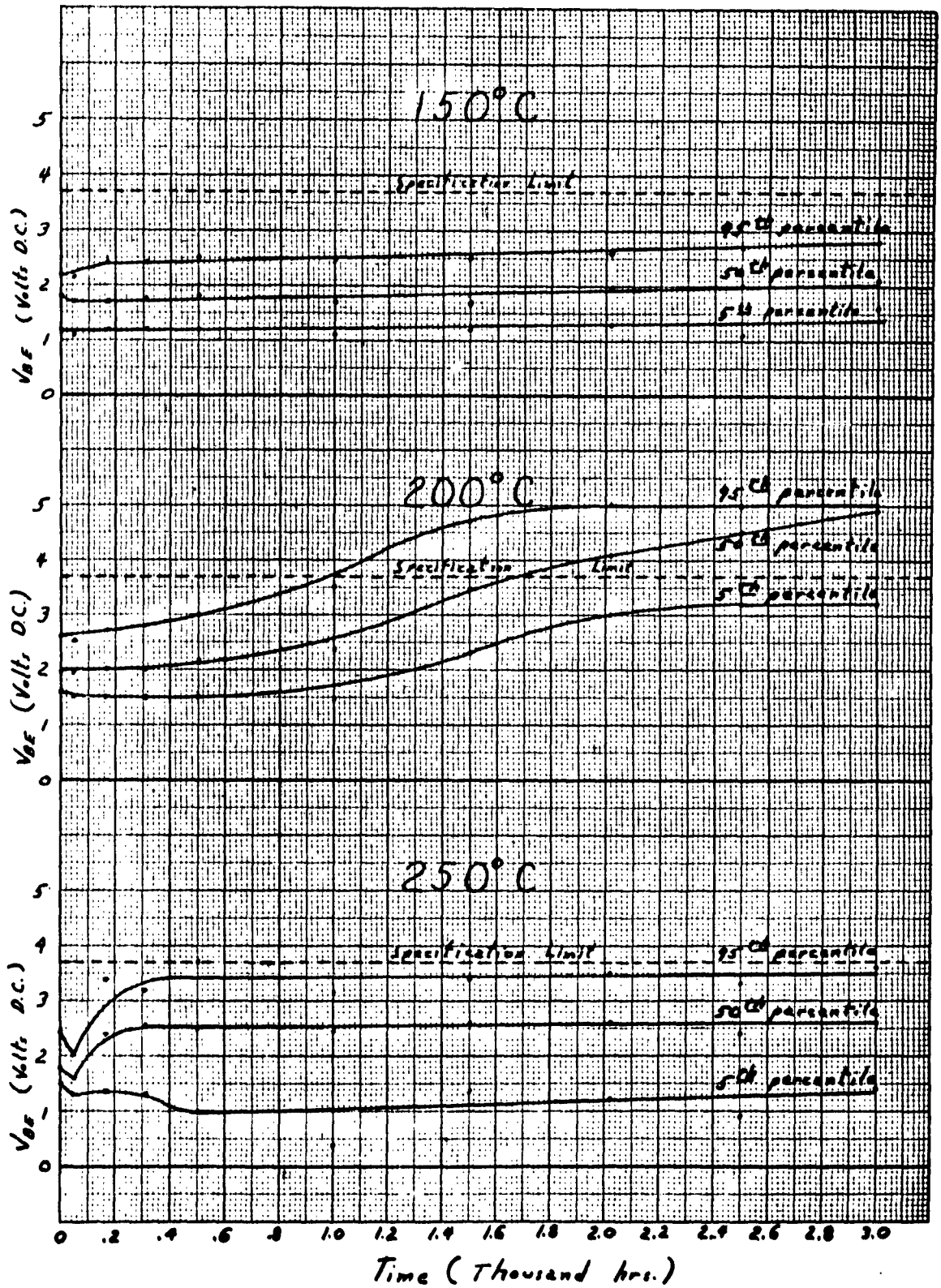
150°C
Specification Limit
95th percentile
50th percentile
5th percentile
200°C
Specification Limit
95th percentile
50th percentile
5th percentile
250°C
Specification Limit
95th percentile
50th percentile
5th percentile
VBE (Volts D.C.)
0
1
2
3
4
5
0 .2 .4 .6 .8 1.0 1.2 1.4 1.6 1.8 2.0 2.2 2.4 2.6 2.8 3.0
Time (Thousand hrs.)

V_{BE} vs Time

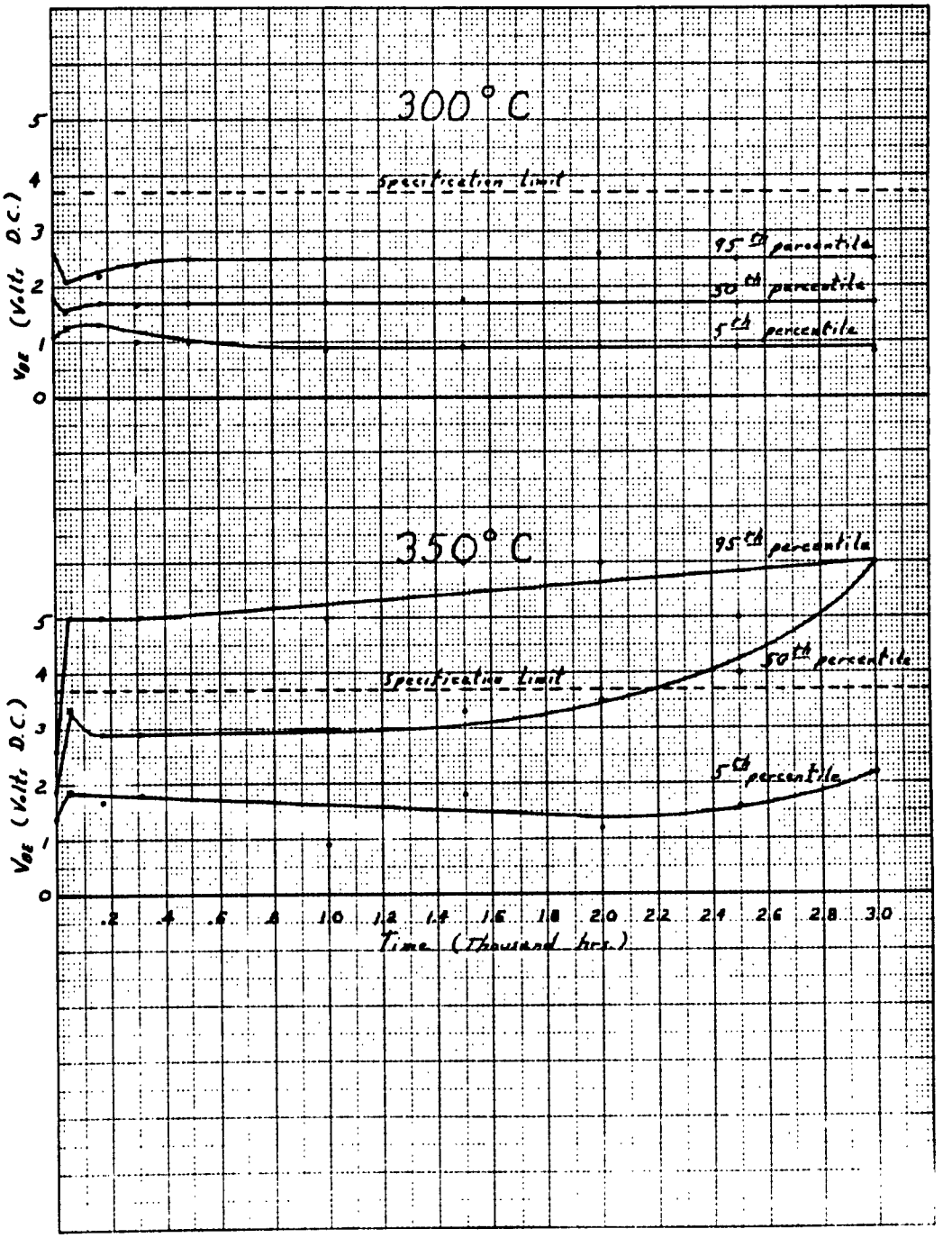
300° C
Specification Limit
95th percentile
50th percentile
5th percentile
VBE (Volts D.C.)
350° C
Specification Limit
95th percentile
50th percentile
5th percentile
VBE (Volts D.C.)
0
1
2
3
4
5
.2
.4
.6
.8
1.0
1.2
1.4
1.6
1.8
2.0
2.2
2.4
2.6
2.8
3.0
Time (Thousand hrs.)

Gain VS. Time

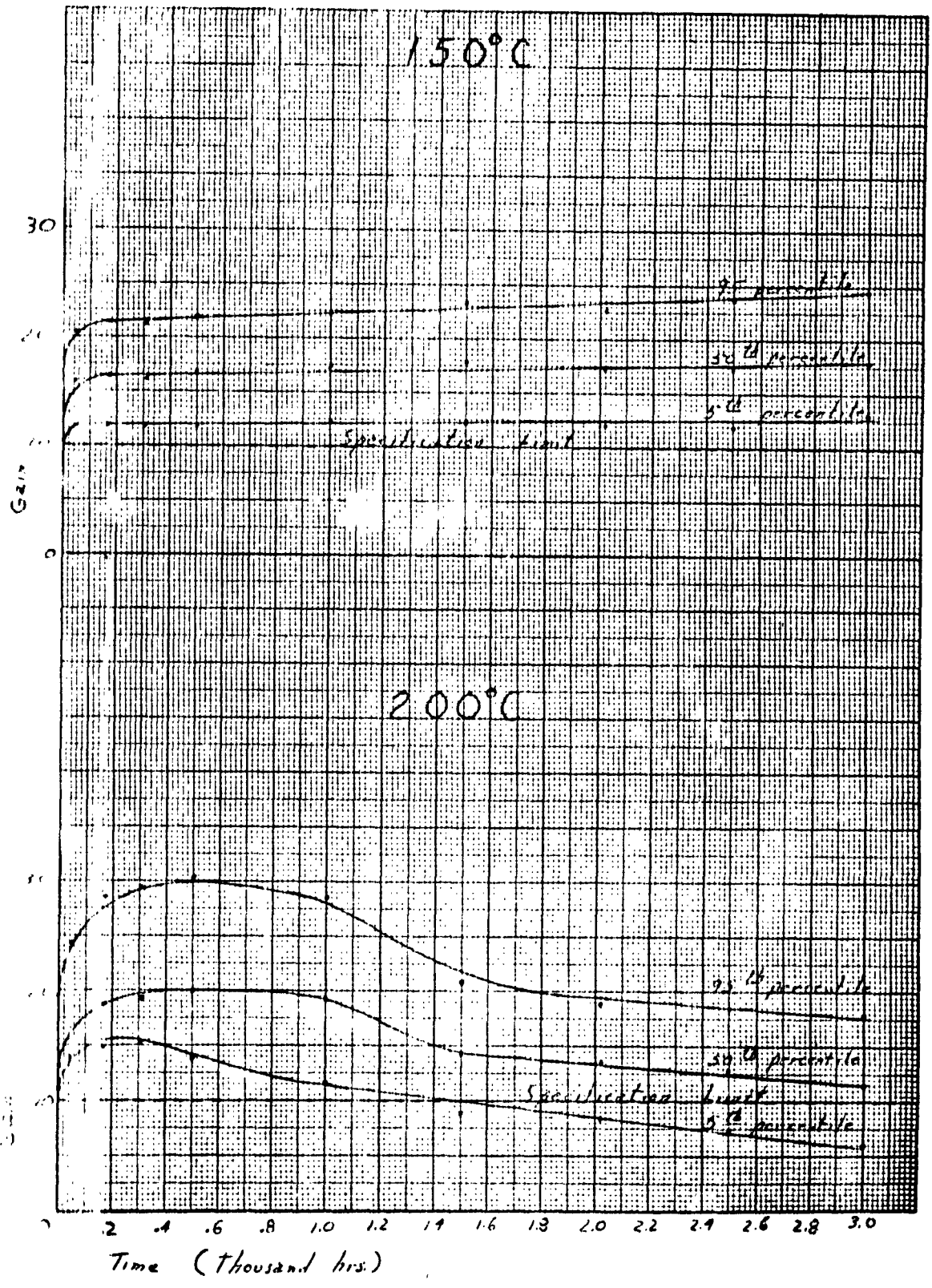
150°C
200°C
30
0
Gain
95 th percentile
50 th percentile
5 th percentile
Specification Limit
.2
.4
.6
.8
1.0
1.2
1.4
1.6
1.8
2.0
2.2
2.4
2.6
2.8
3.0
Time (thousand hrs.)

Gain Vs. Time

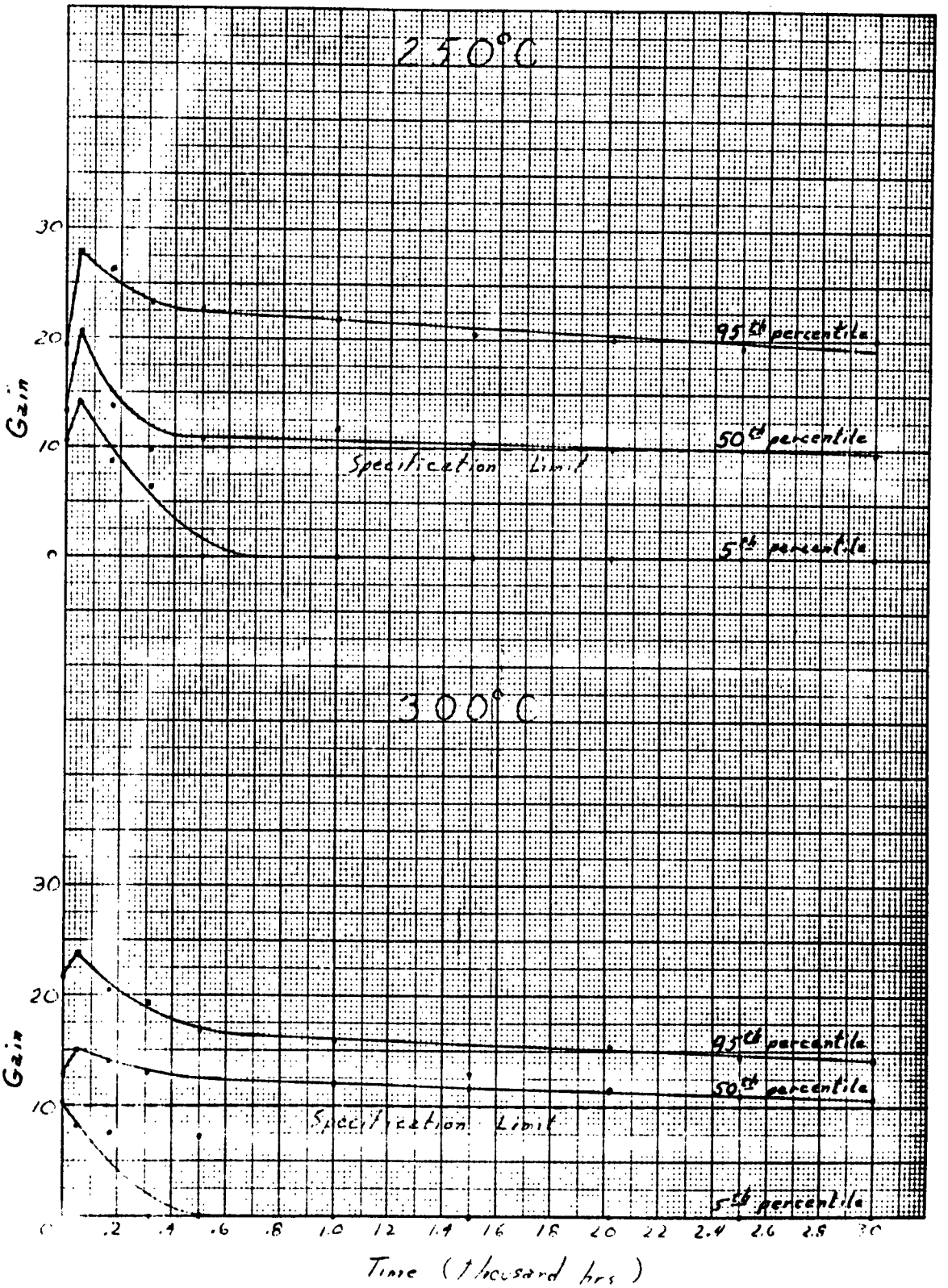
250°C
95th percentile
50th percentile
Specification Limit
5th percentile
300°C
95th percentile
50th percentile
Specification Limit
5th percentile
Gain
Gain
30
20
10
0
30
20
10
0
.2
.4
.6
.8
1.0
1.2
1.4
1.6
1.8
2.0
2.2
2.4
2.6
2.8
3.0
Time (Thousand hrs)

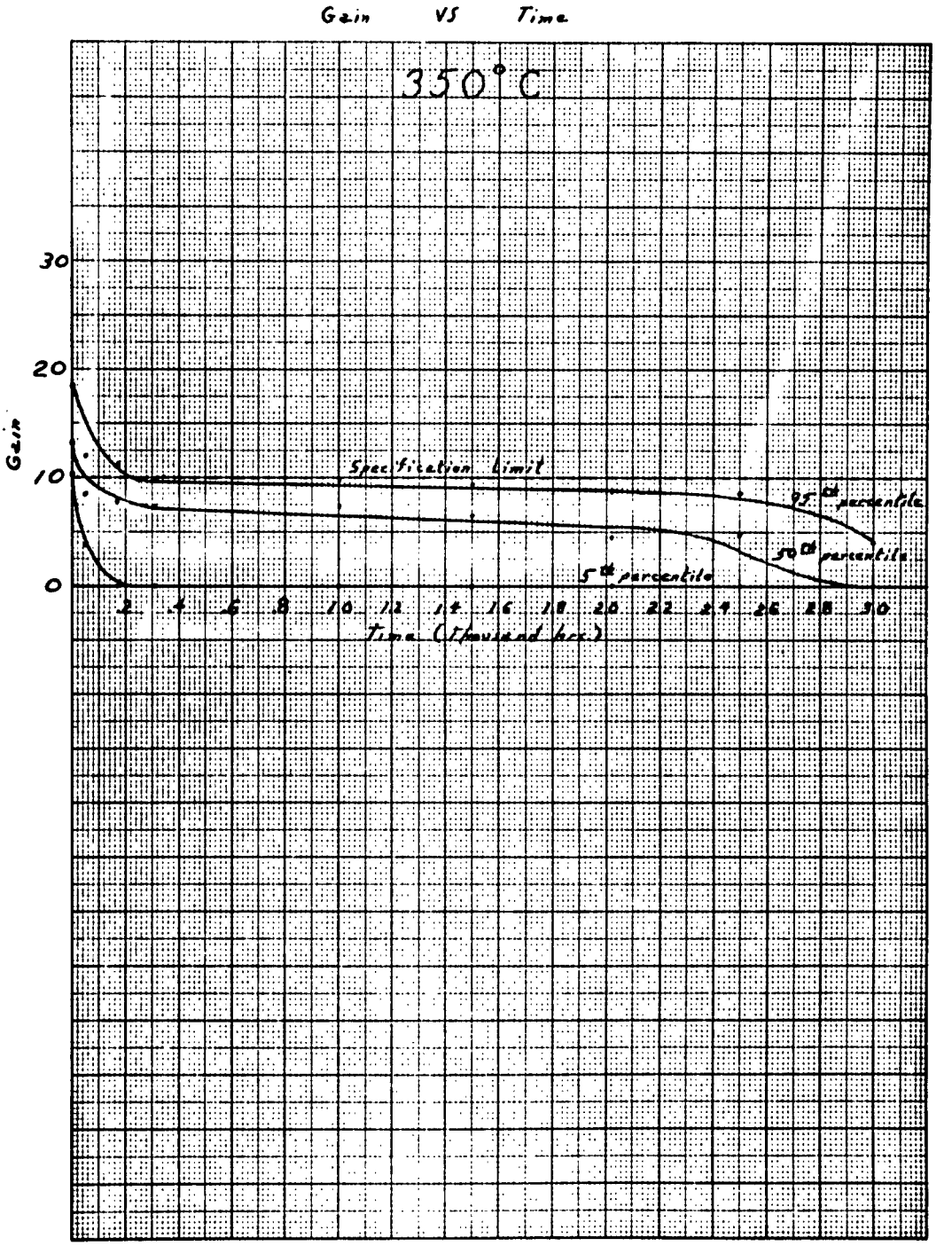
Gain VS Time
350°C
Gain
30
20
10
0
Specification Limit
95th percentile
50th percentile
5th percentile
.2 .4 .6 .8 1.0 1.2 1.4 1.6 1.8 2.0 2.2 2.4 2.6 2.8 3.0
Time (thousand hrs.)

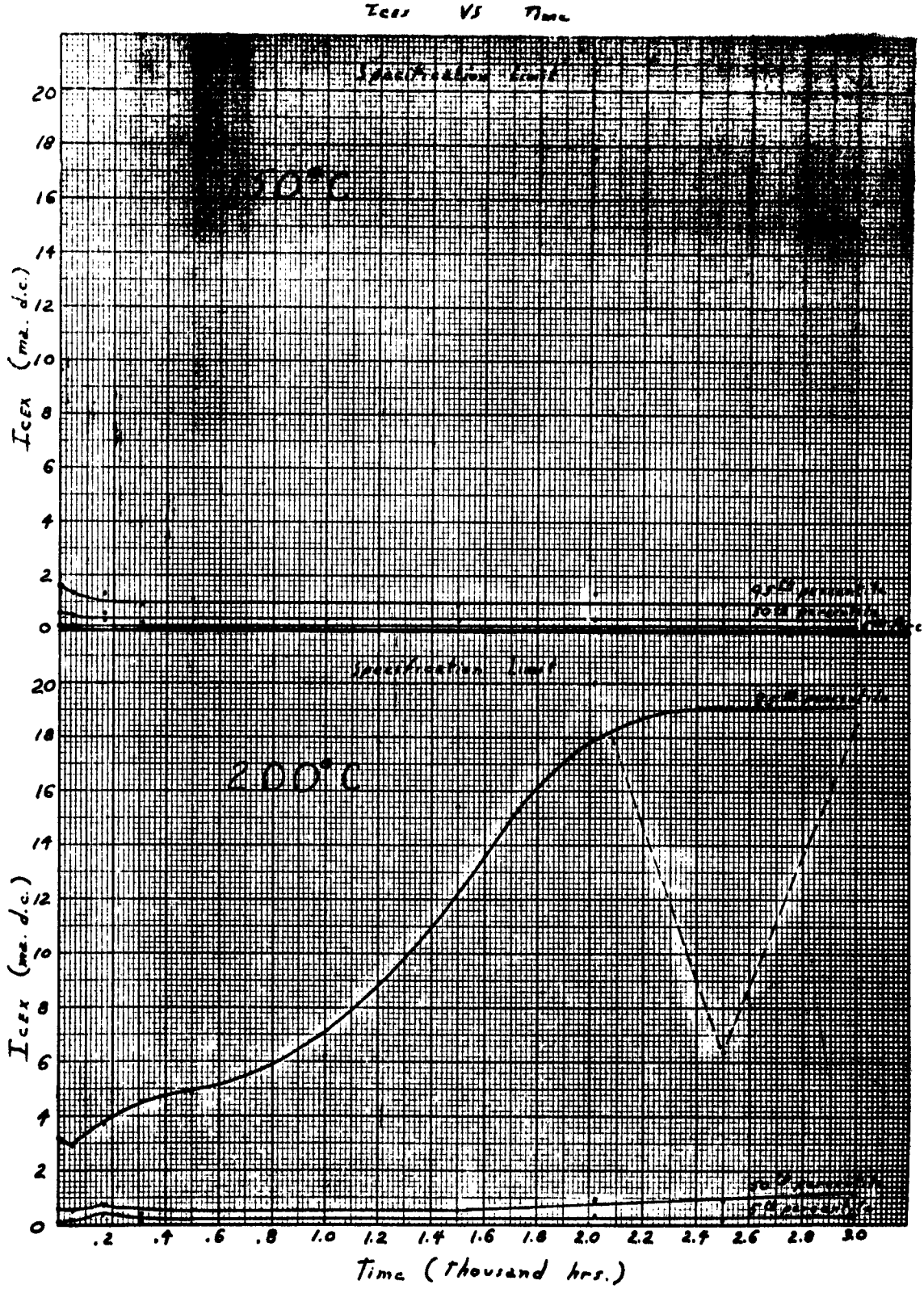
ICES VS Time
Specification Limit
200°C
ICEX (ma. d.c.)
Time (Thousand hrs.)
.2
.4
.6
.8
1.0
1.2
1.4
1.6
1.8
2.0
2.2
2.4
2.6
2.8
3.0
0
2
4
6
8
10
12
14
16
18
20

I_{CEX} VS Time

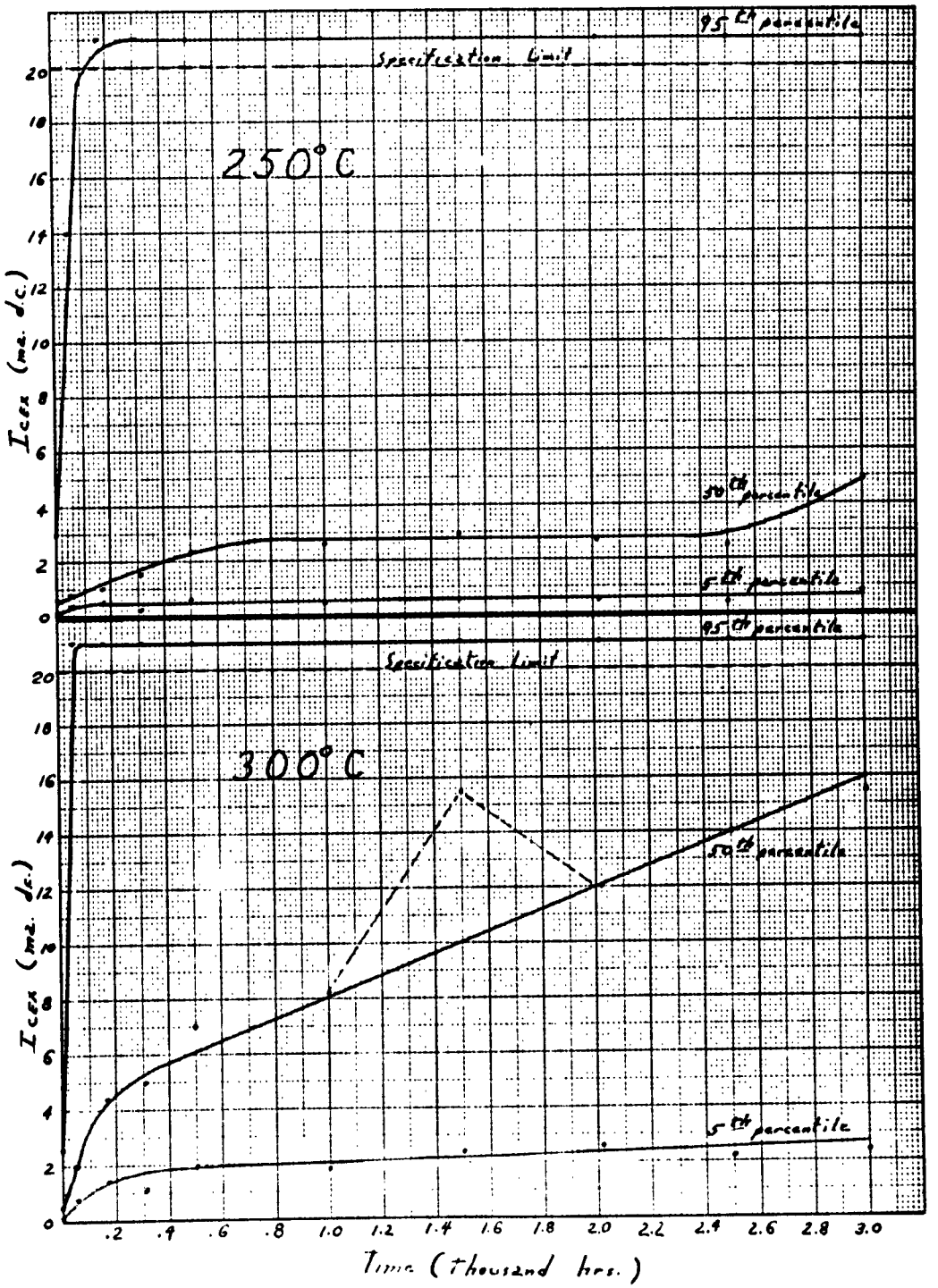
95th percentile
Specification Limit
250°C
I_{CEX} (ma. d.c.)
50th percentile
5th percentile
95th percentile
Specification Limit
300°C
I_{CEX} (ma. d.c.)
50th percentile
5th percentile
0 2 4 6 8 10 12 14 16 18 20
.2 .4 .6 .8 1.0 1.2 1.4 1.6 1.8 2.0 2.2 2.4 2.6 2.8 3.0
Time (Thousand hrs.)

I_{CEX} VS Time

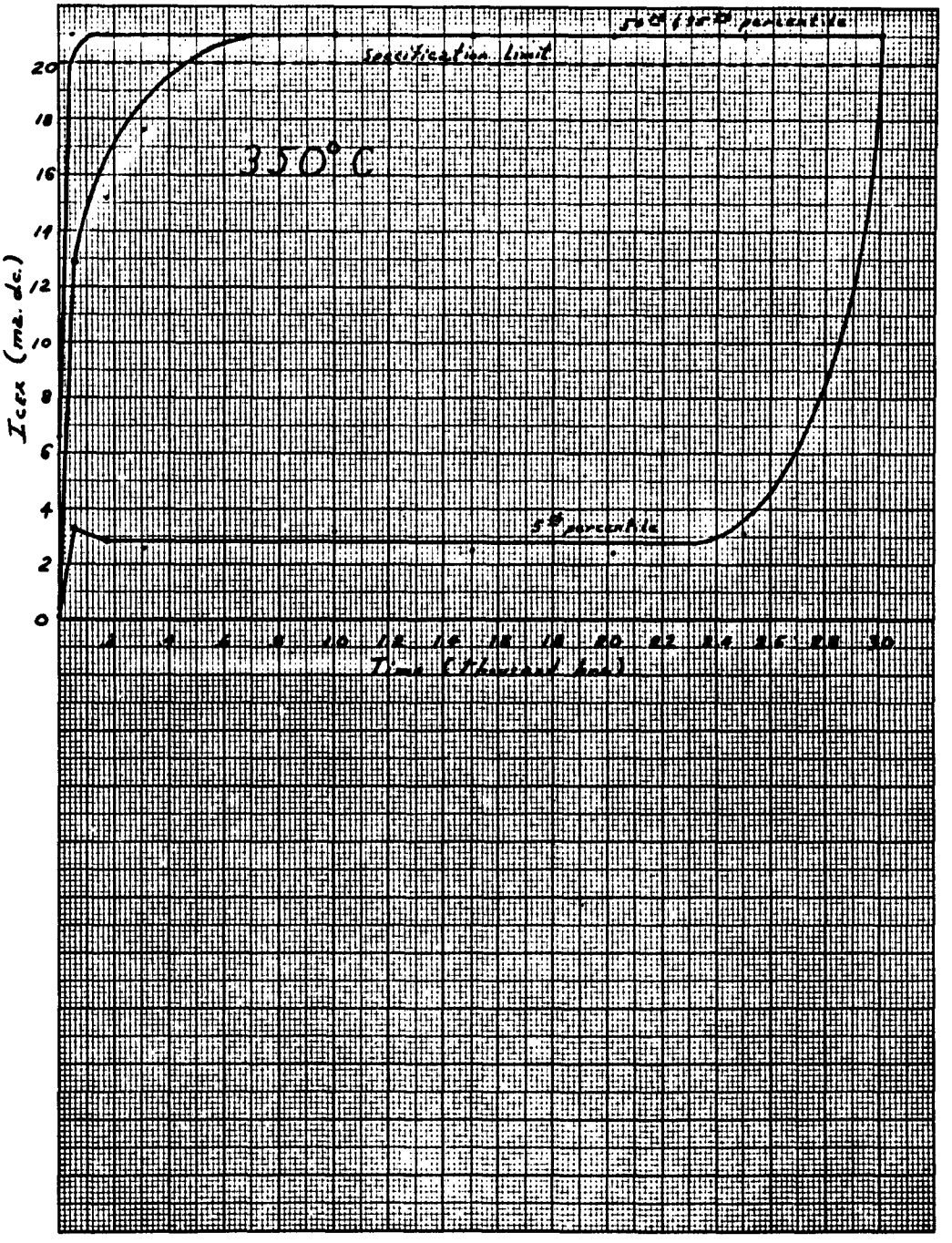
95th percentile
Specification Limit
350° C
5th percentile
I_{CEX} (ma. dc.)
0
2
4
6
8
10
12
14
16
18
20
Time (thousand hrs.)

V_{BE} VS. Time (50th percentiles)

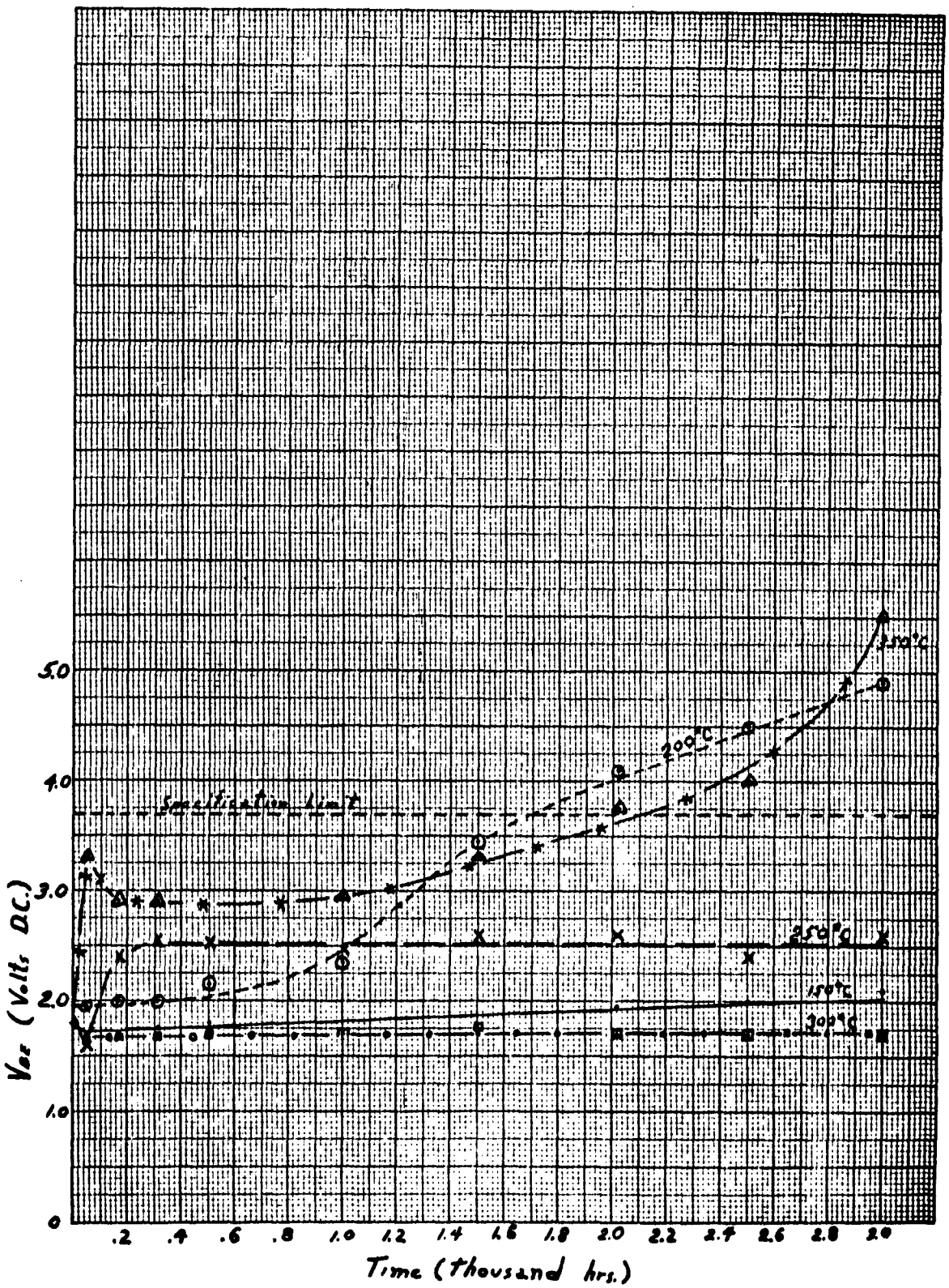

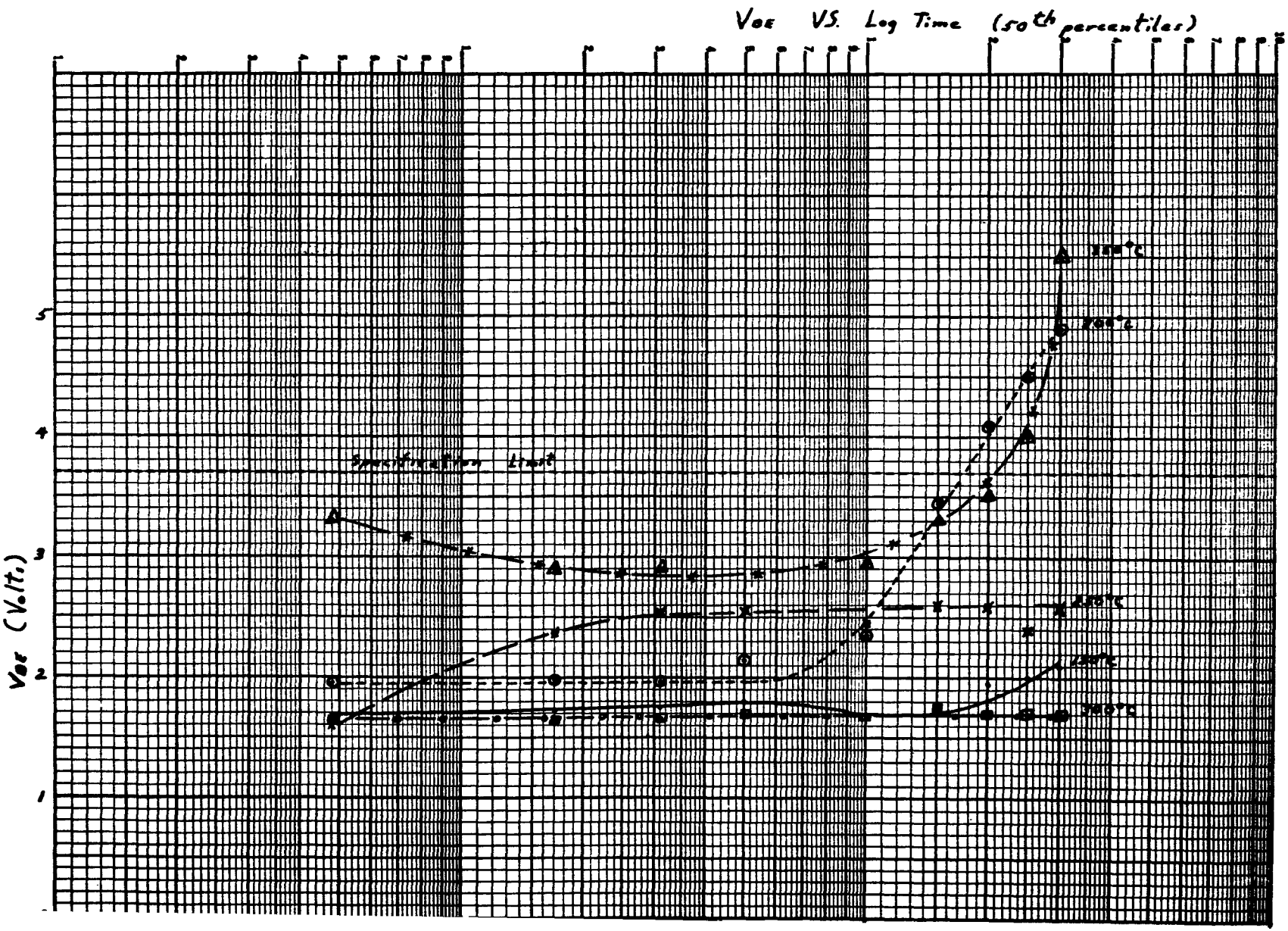
VOE VS. Log Time (50th percentiles)
VOE (Volts)
5
4
3
2
1
Specification Limit
385°C
360°C
340°C
320°C
300°C

-0/-

Log V_{BE} VS. Time (50th percentiles)

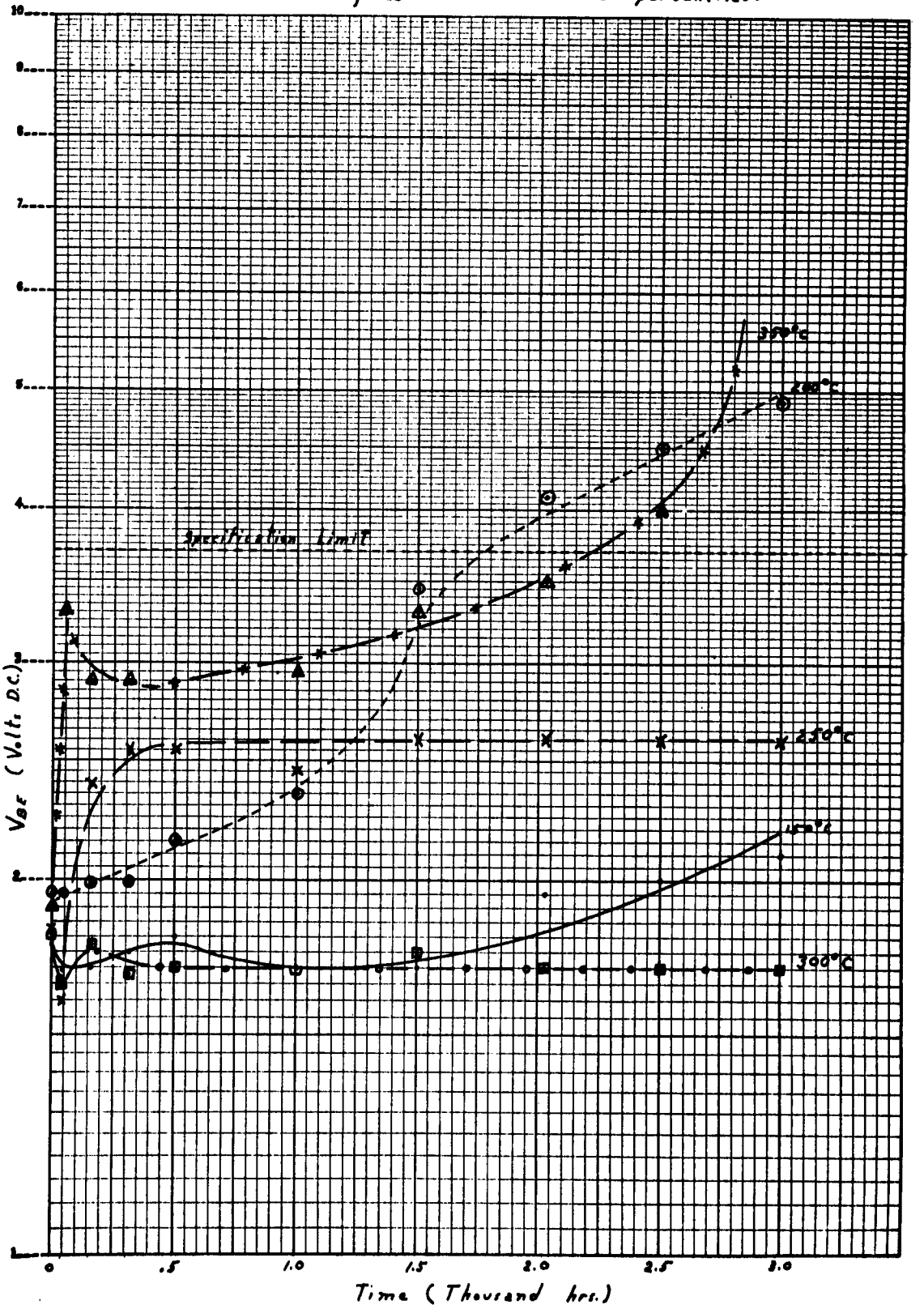

$\frac{V_{BE}\ Reading}{V_{BE}\ Reading\ @\ t_o}$ V.S. Time (50th percentiles)

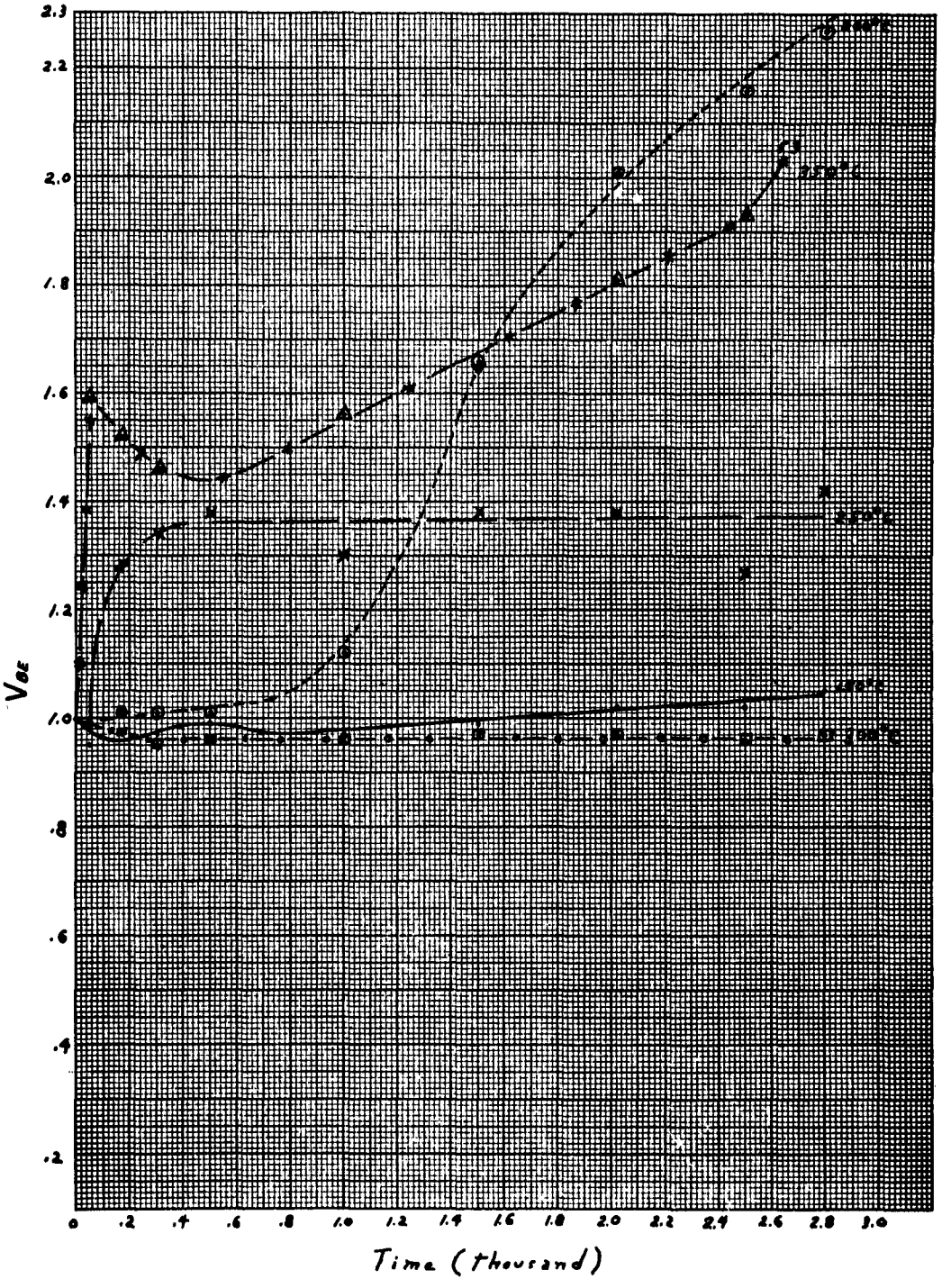

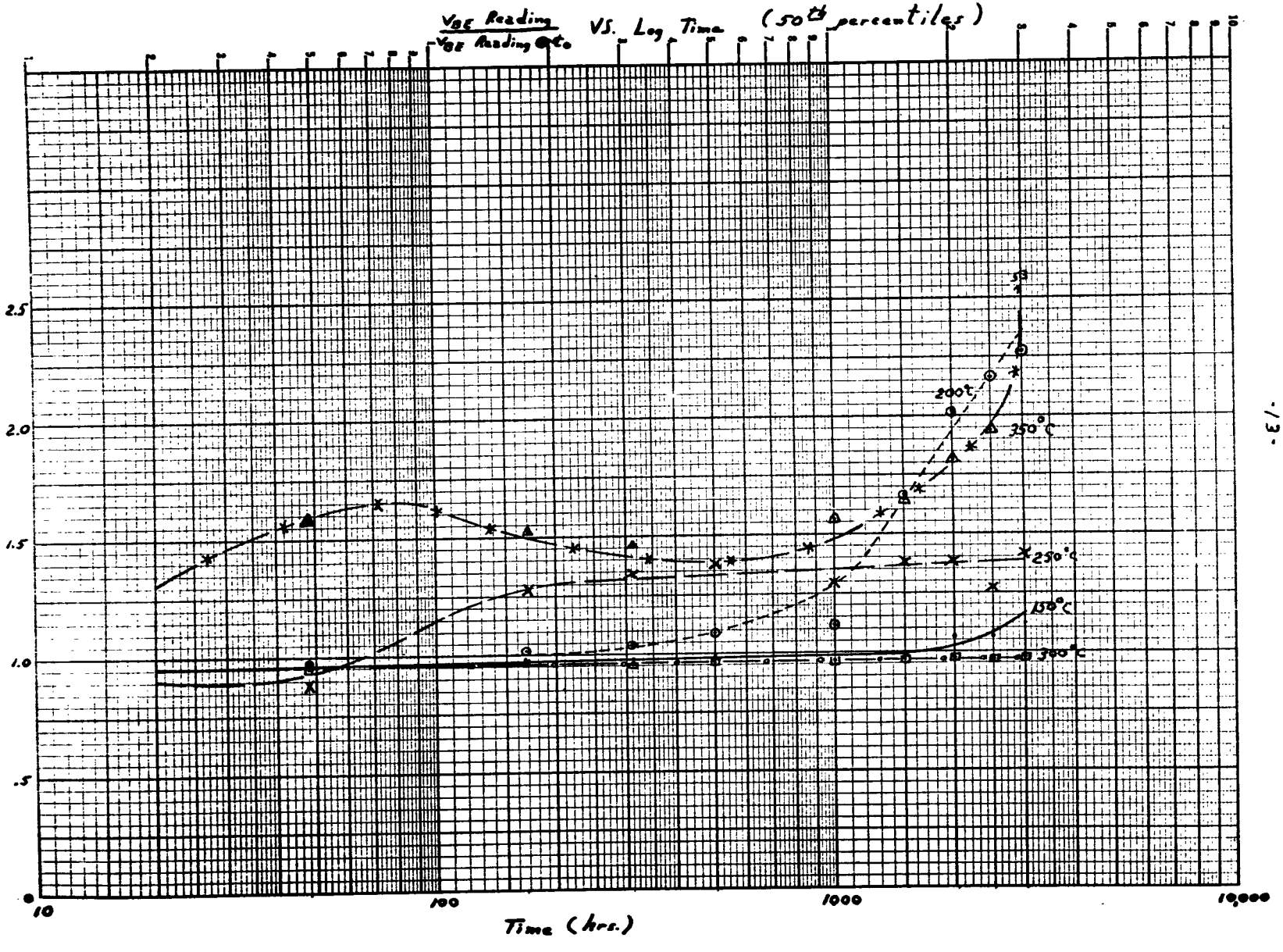
$\frac{V_{BE}\ Reading}{V_{BE}\ Reading\ @\ t_o}$ VS. Log Time (50th percentiles)
2.5
2.0
1.5
1.0
.5
0
10
100
1000
10,000
Time (hrs.)
200°C
350°C
250°C
150°C
300°C

Icex VS. Time (50th percentiles)

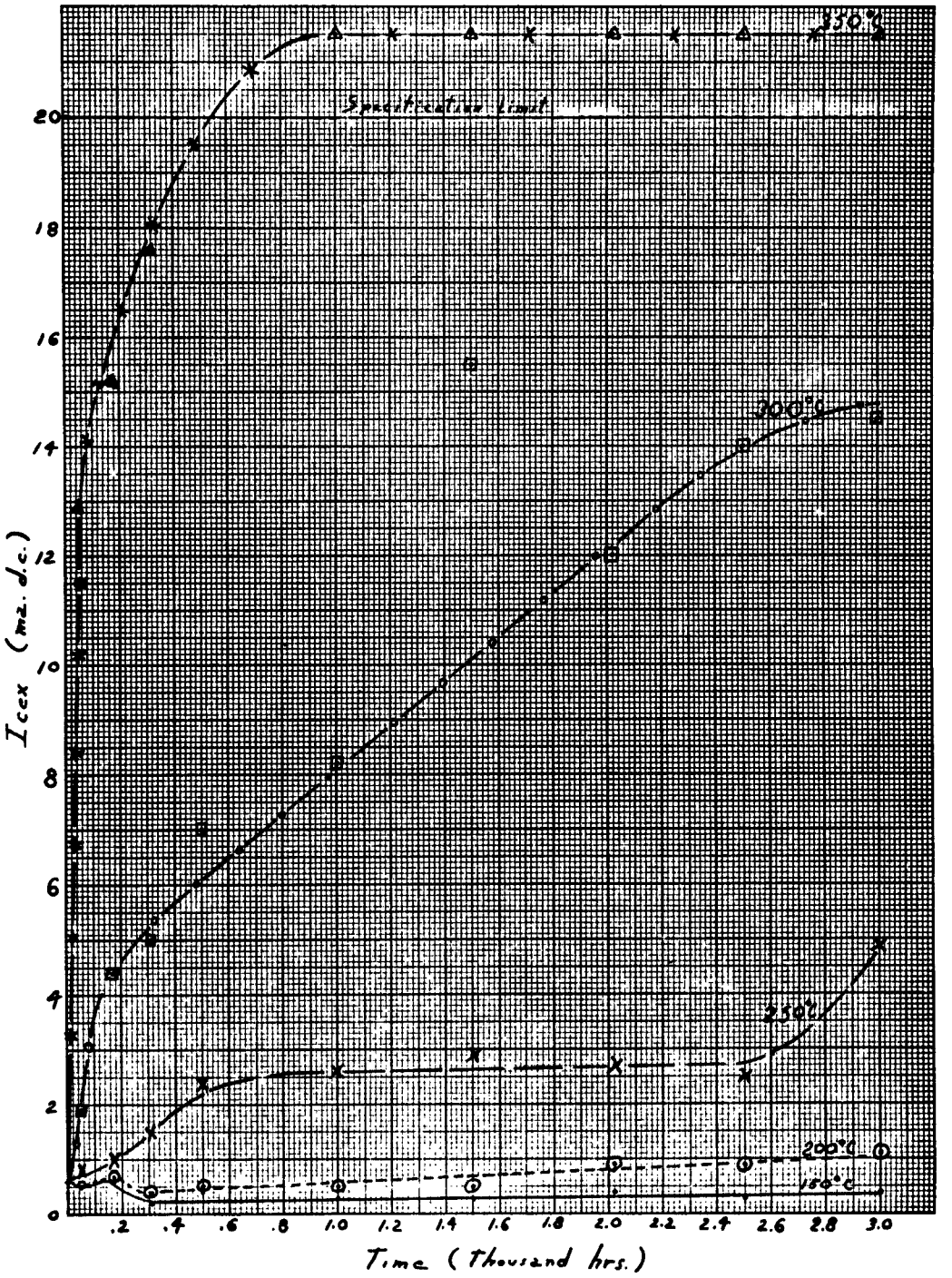

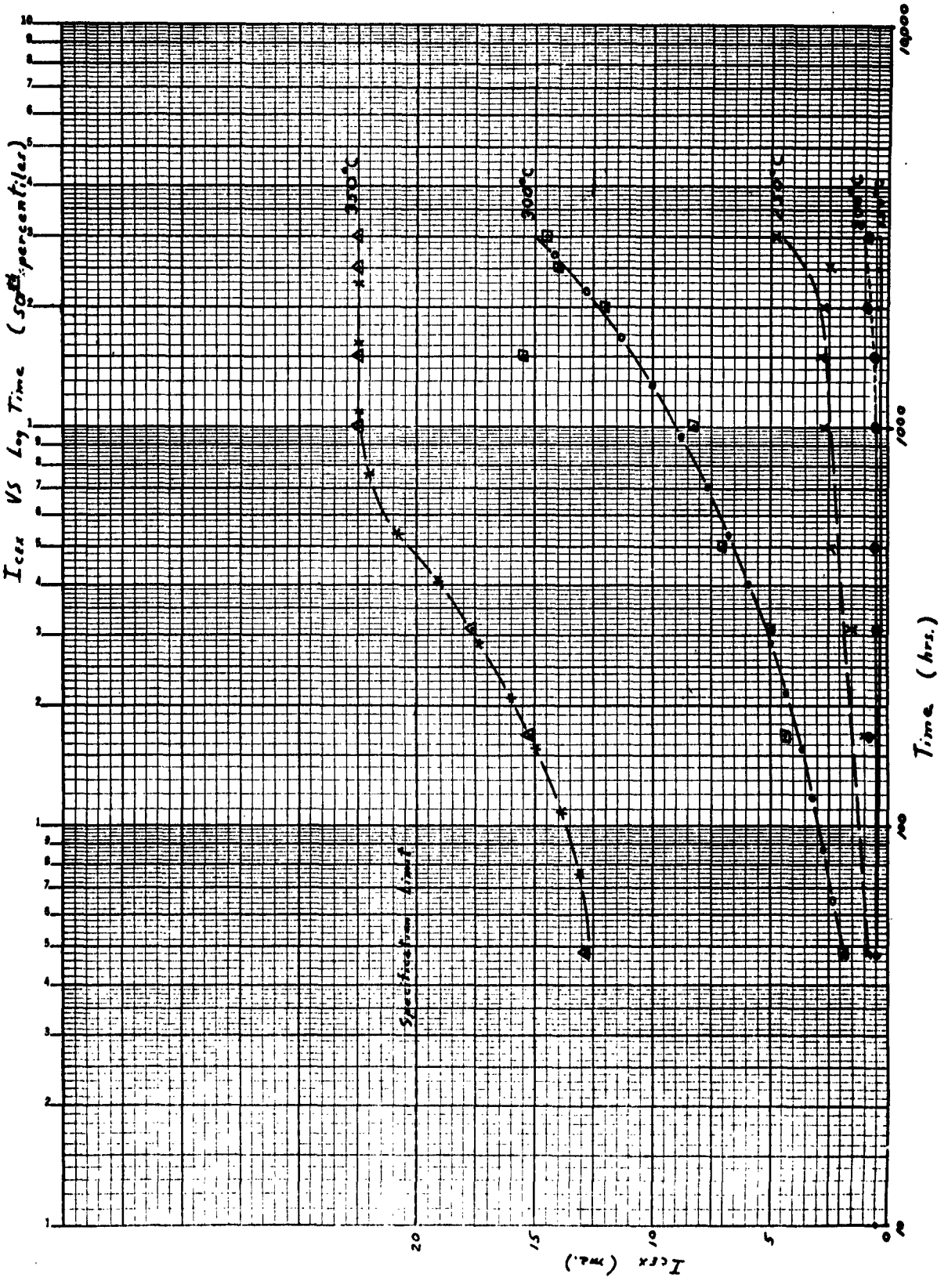
I_{CEX} Vs Log Time (50th percentiles)
350°C
300°C
250°C
Specification Limit
I_{CEX} (mA.)
Time (hrs.)
20
15
10
5
0
1
2
3
4
5
6
7
8
9
10
100
1000
10000

Log I_{cex} VS Time (50th percentiles)

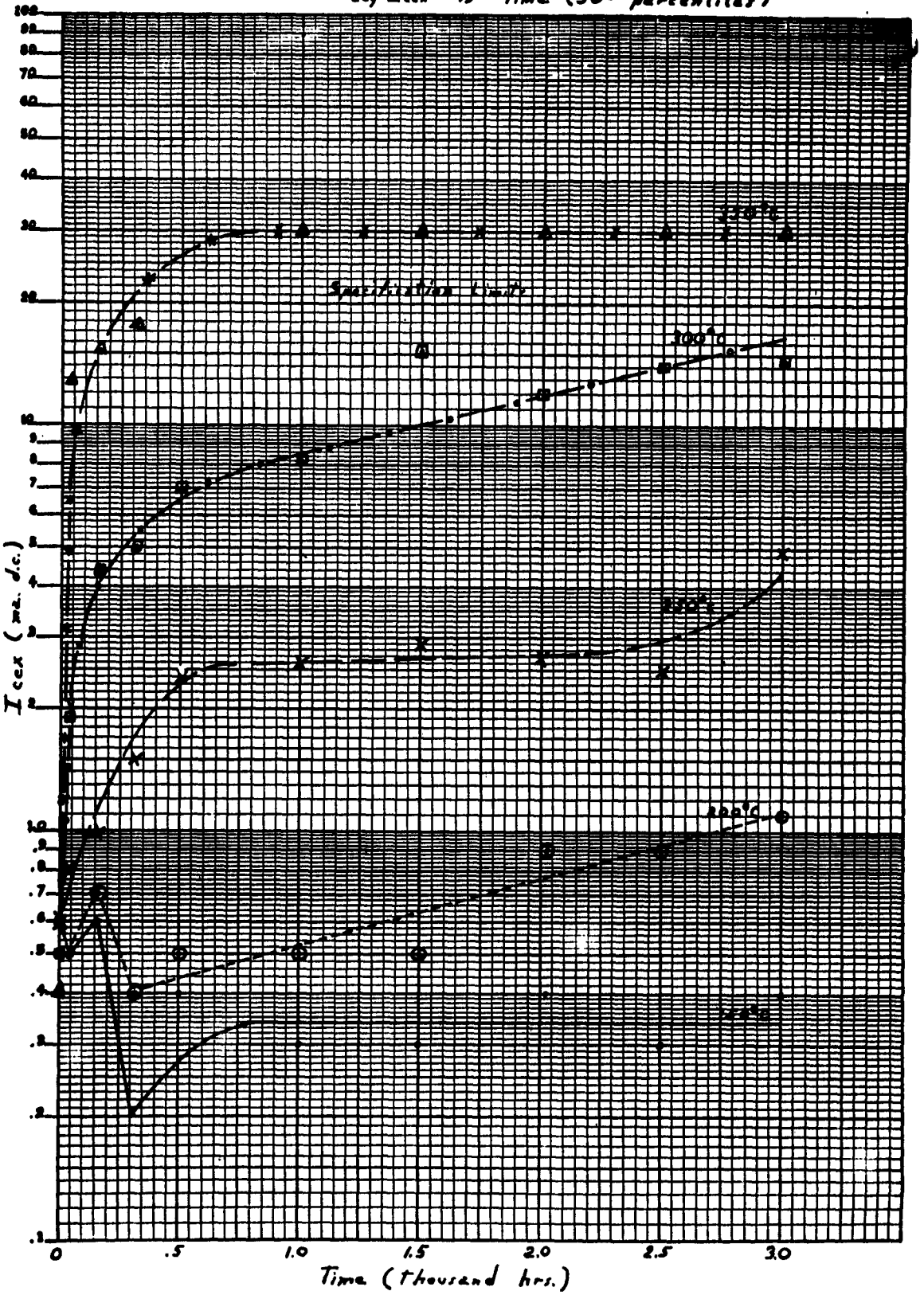

$\frac{I_{CEX}\ Reading}{I_{CEX}\ Reading\ @\ T_0}$ VS. Time. (50^{th} percentiles)

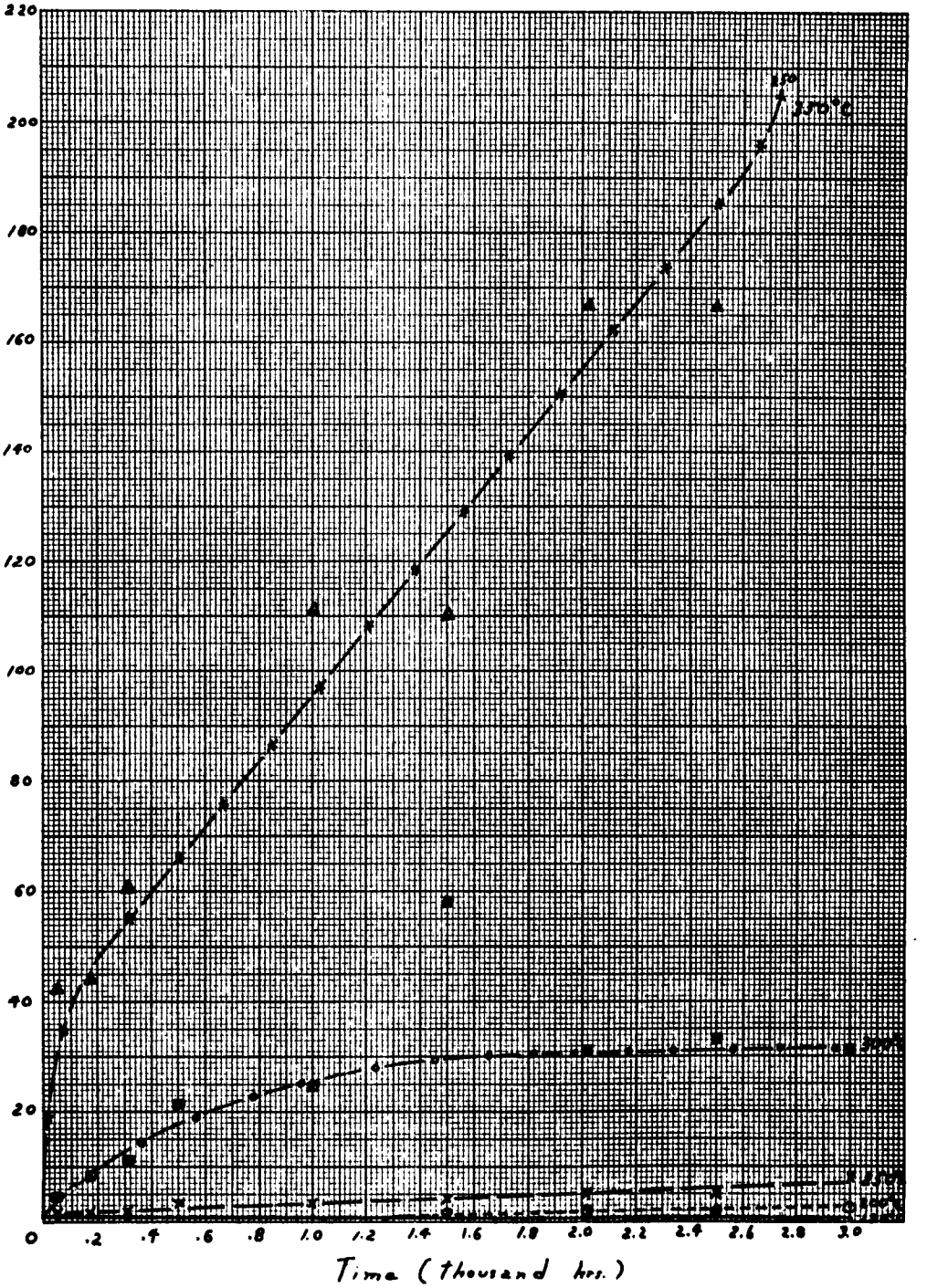

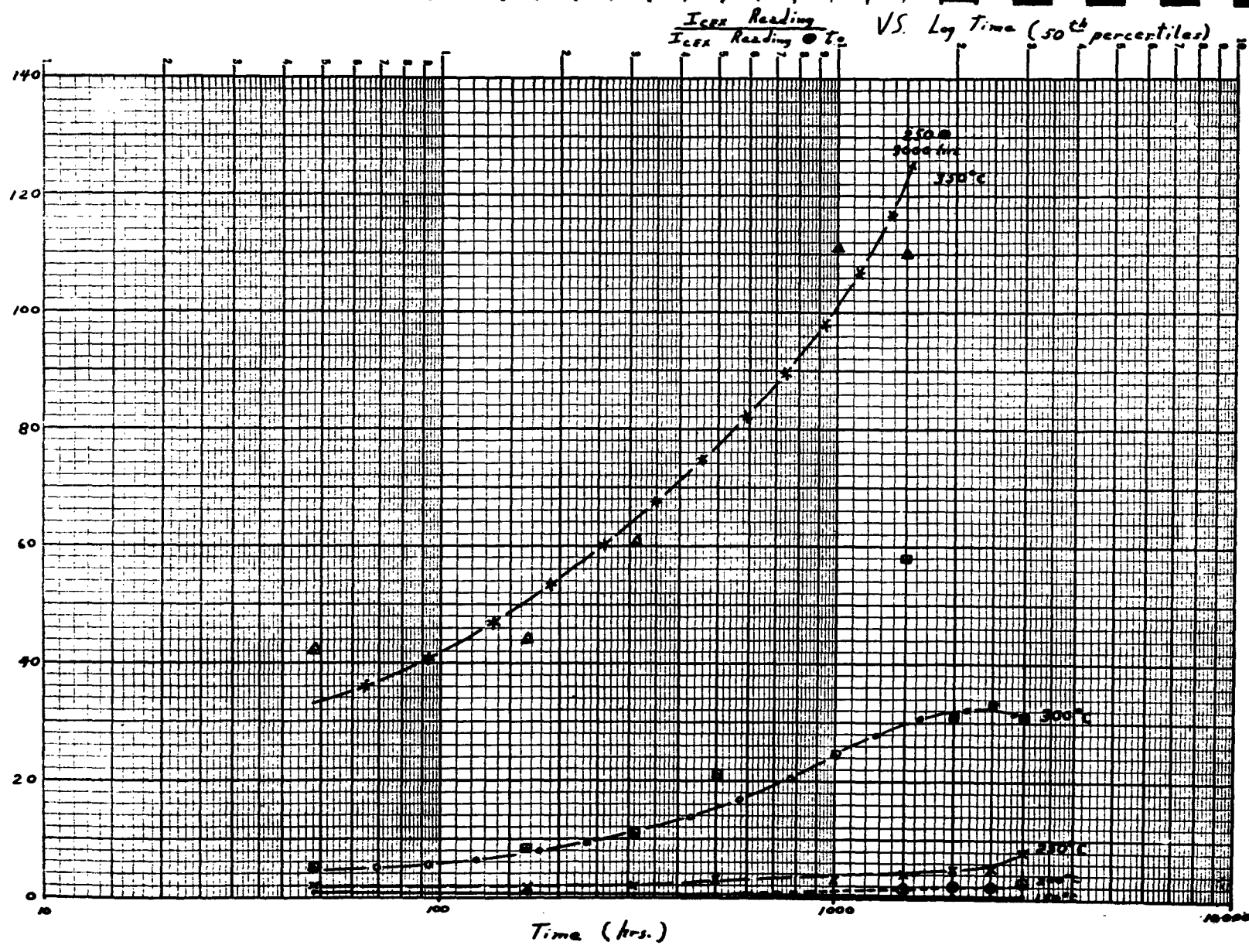
$\frac{I_{CES}\ Reading}{I_{CES}\ Reading\ @\ t_o}$ VS. Log Time (50th percentiles)
140
120
100
80
60
40
20
0
10
100
1000
10000
Time (hrs.)
250 @ 3000 hrs
350°C
300°C
210°C

Gain VS. Time (50th percentiles)

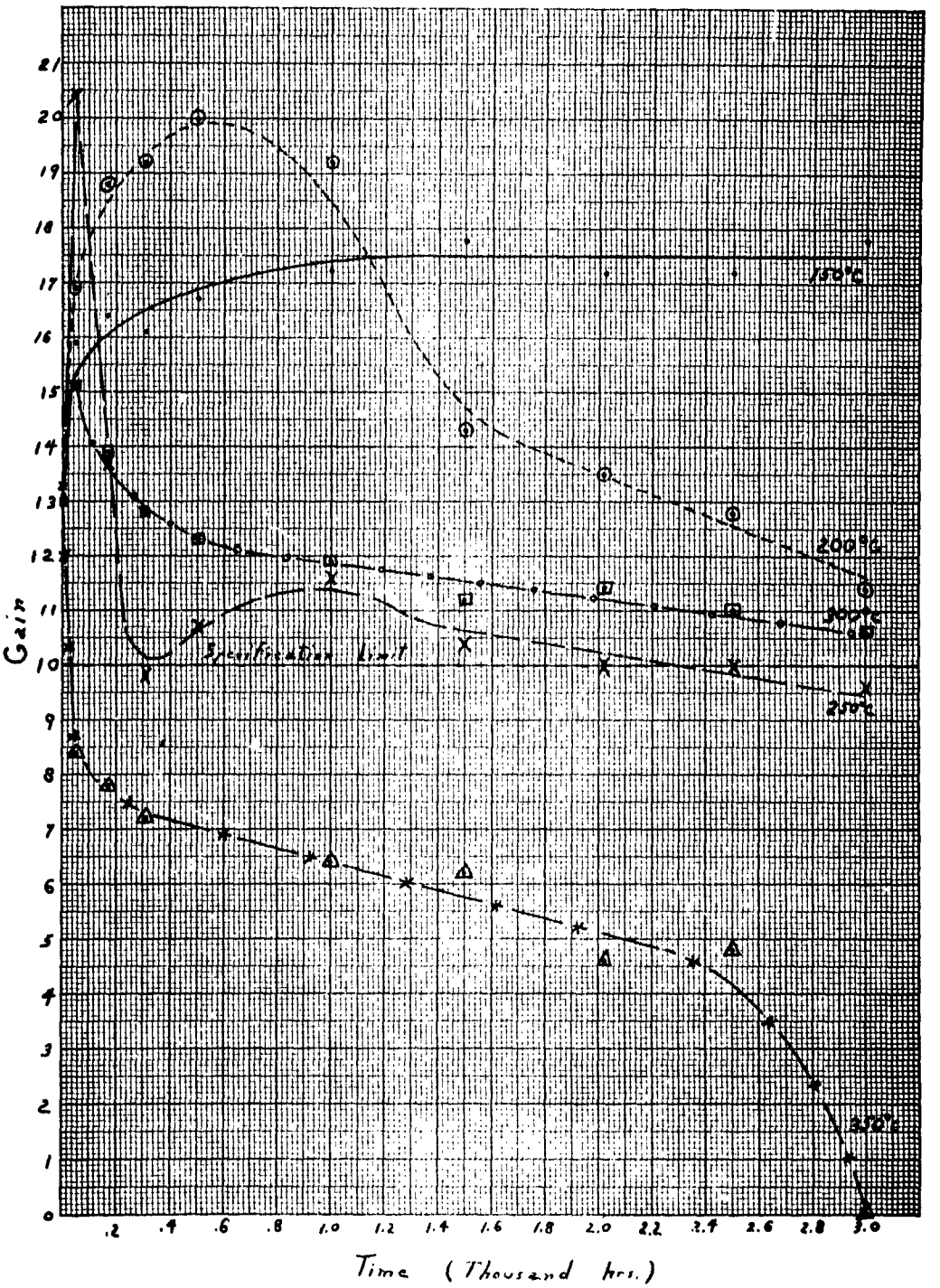

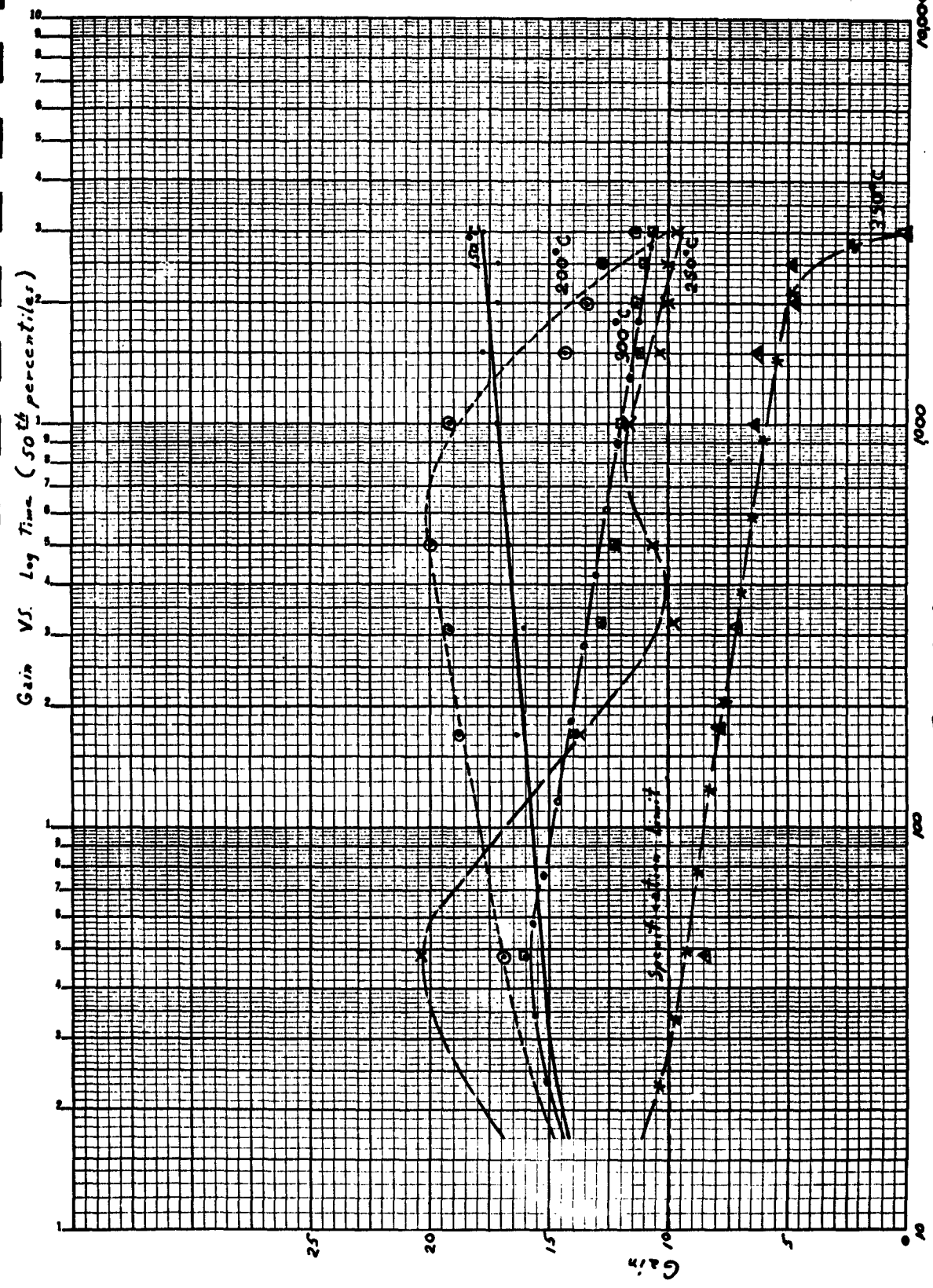
Gain VS. Log Time (50th percentiles)
Gain
Time (hrs.)
150°C
200°C
250°C
300°C
350°C
Specification Limit

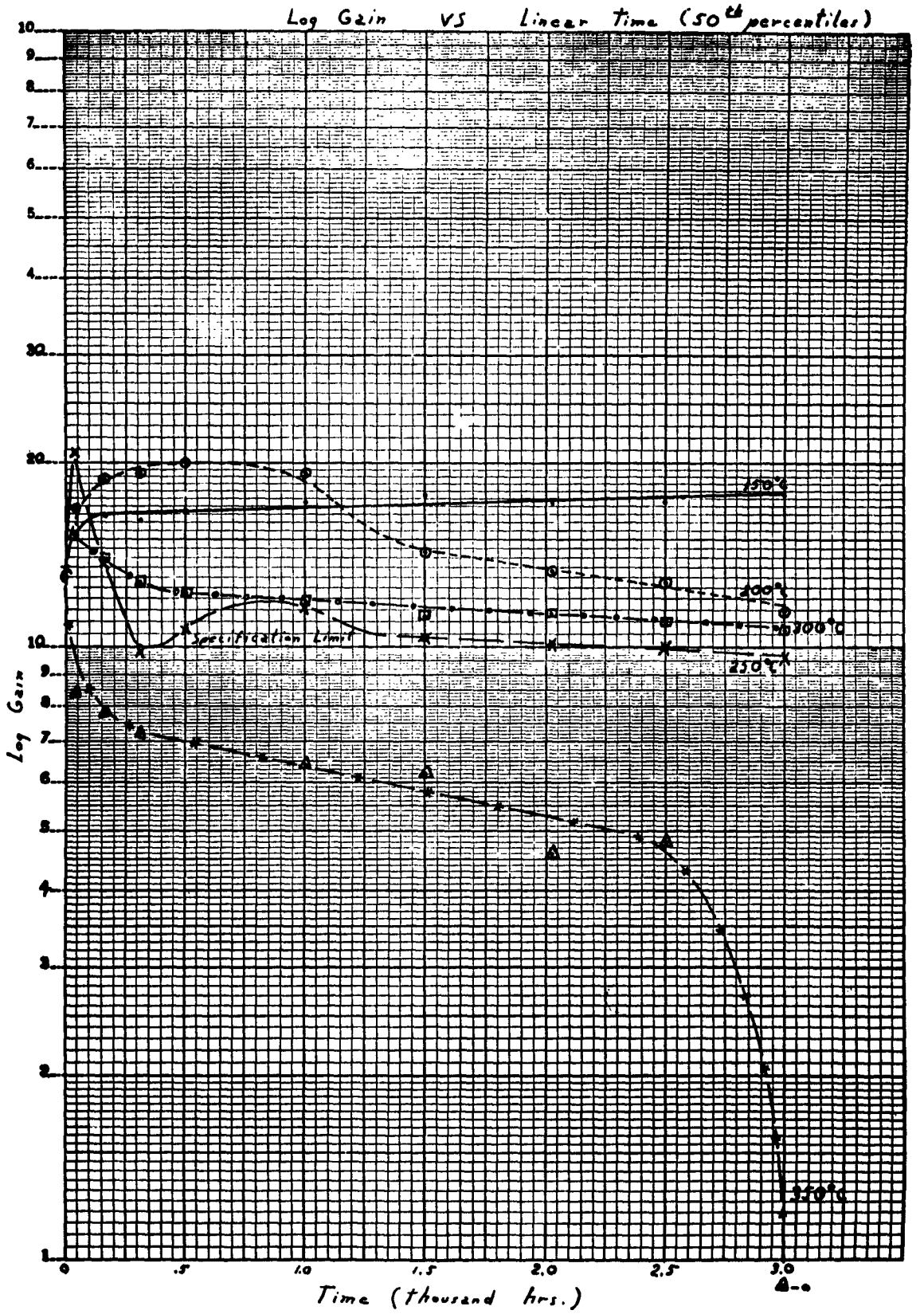
Log Gain VS Linear Time (50th percentiles)
Log Gain
Time (thousand hrs.)
Specification Limit
150°C
200°C
300°C
250°C
350°C
10
9
8
7
6
5
4
3
2
1
20
0
.5
1.0
1.5
2.0
2.5
3.0

$\frac{\text{Gain reading}}{\text{Gain reading @ time 0}}$ VS. Time (50th percentiles)

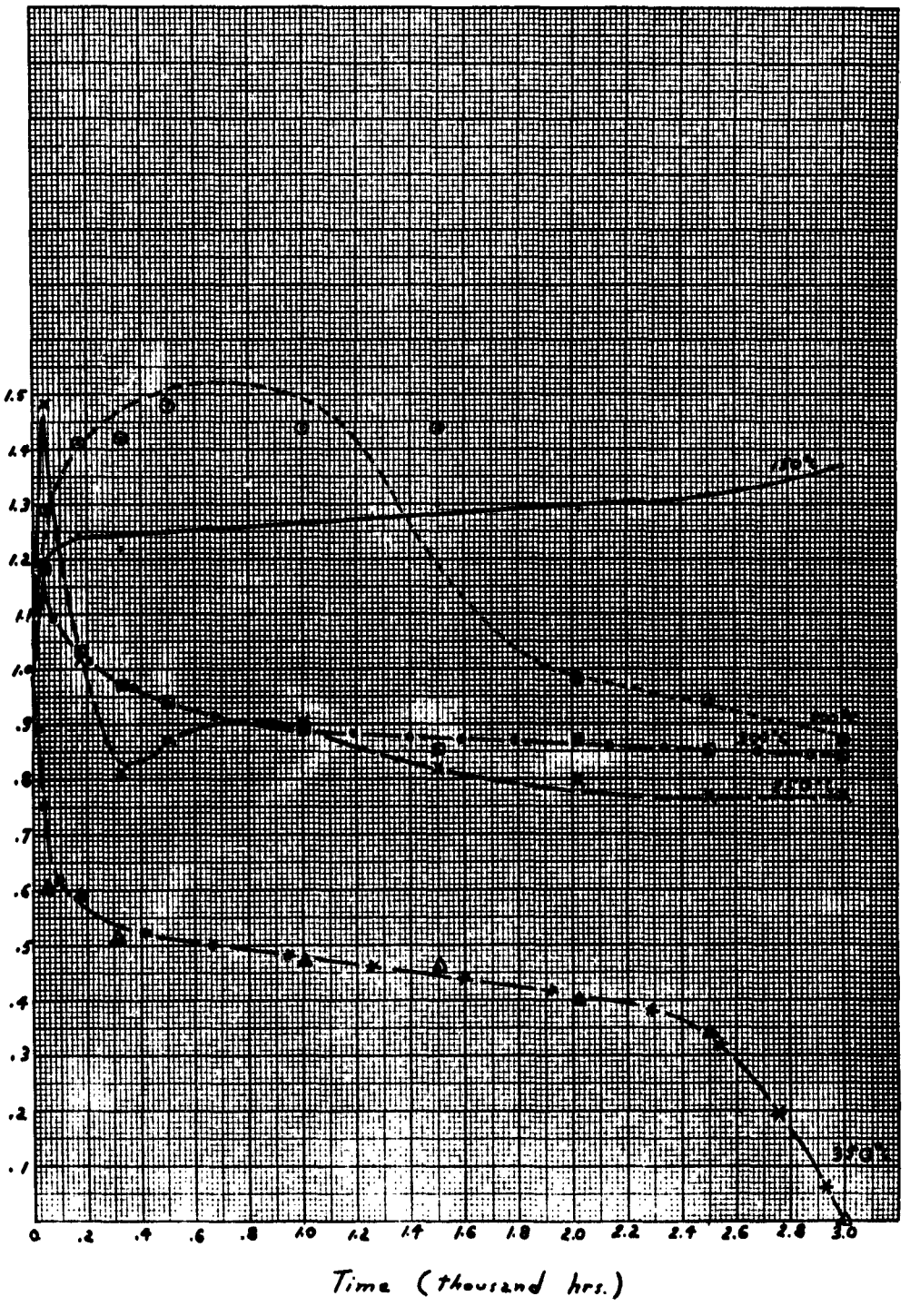

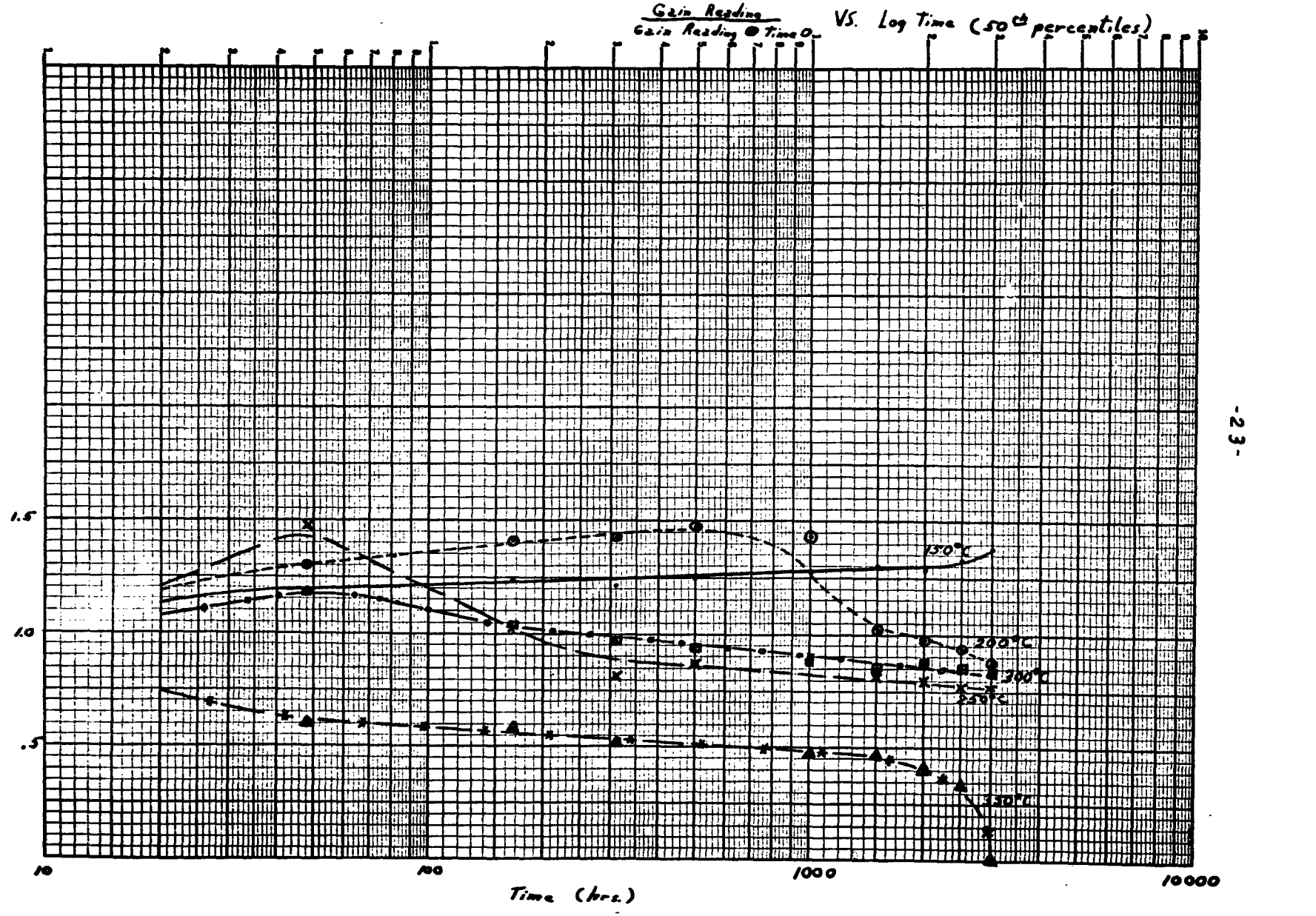
Gain Reading / Gain Reading @ Time 0 VS. Log Time (50th percentiles)
1.5
1.0
.5
10
100
1000
10000
Time (hrs.)
150°C
200°C
300°C
250°C
350°C

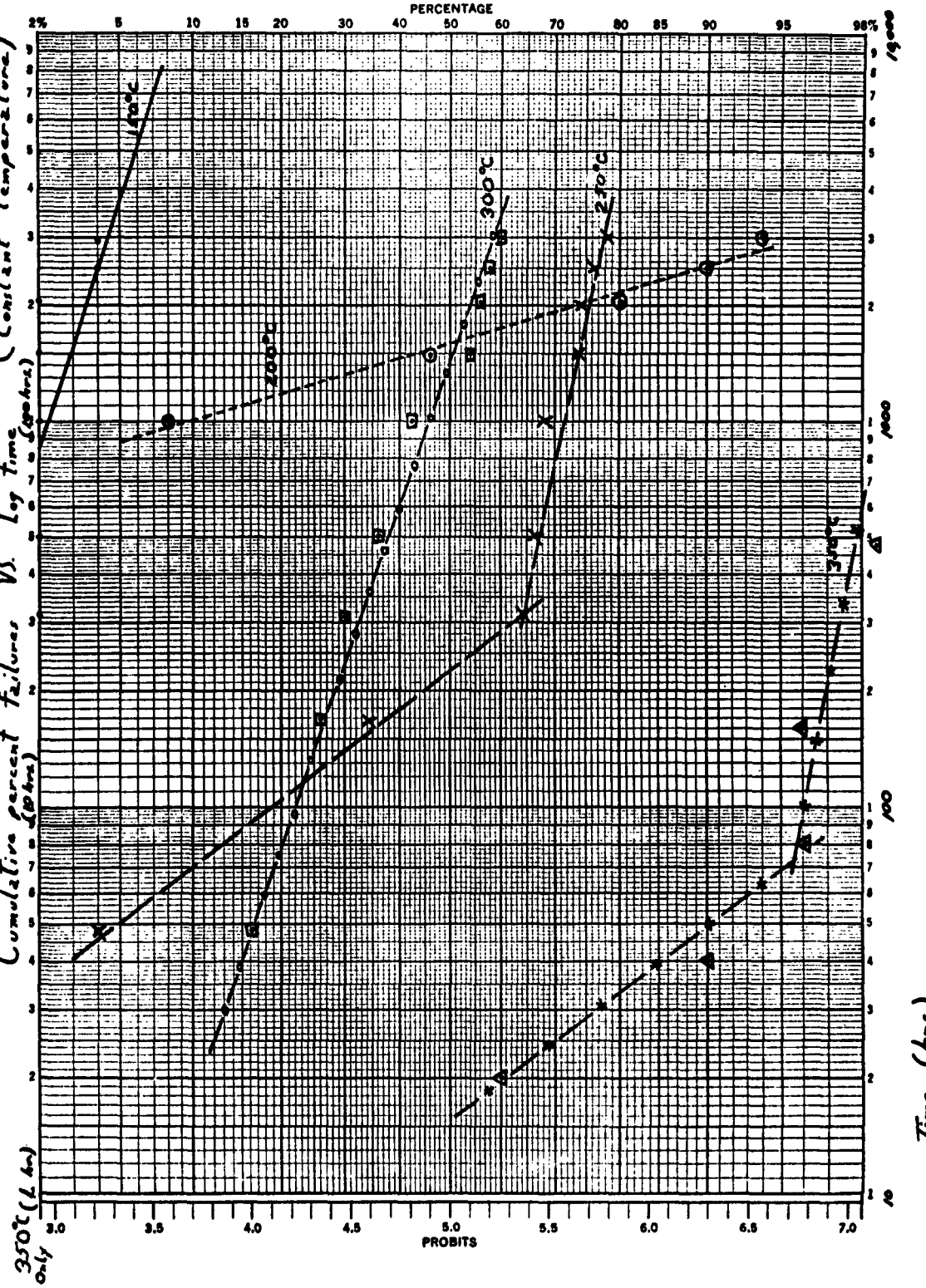
Cumulative percent failures Vs. Log time (Constant temperature)
PERCENTAGE
2% 5 10 15 20 30 40 50 60 70 80 85 90 95 98%
PROBITS
3.0 3.5 4.0 4.5 5.0 5.5 6.0 6.5 7.0
Time (hrs.)
1 10 100 1000
150°C
200°C
300°C
270°C
350°C (1 hr)
only

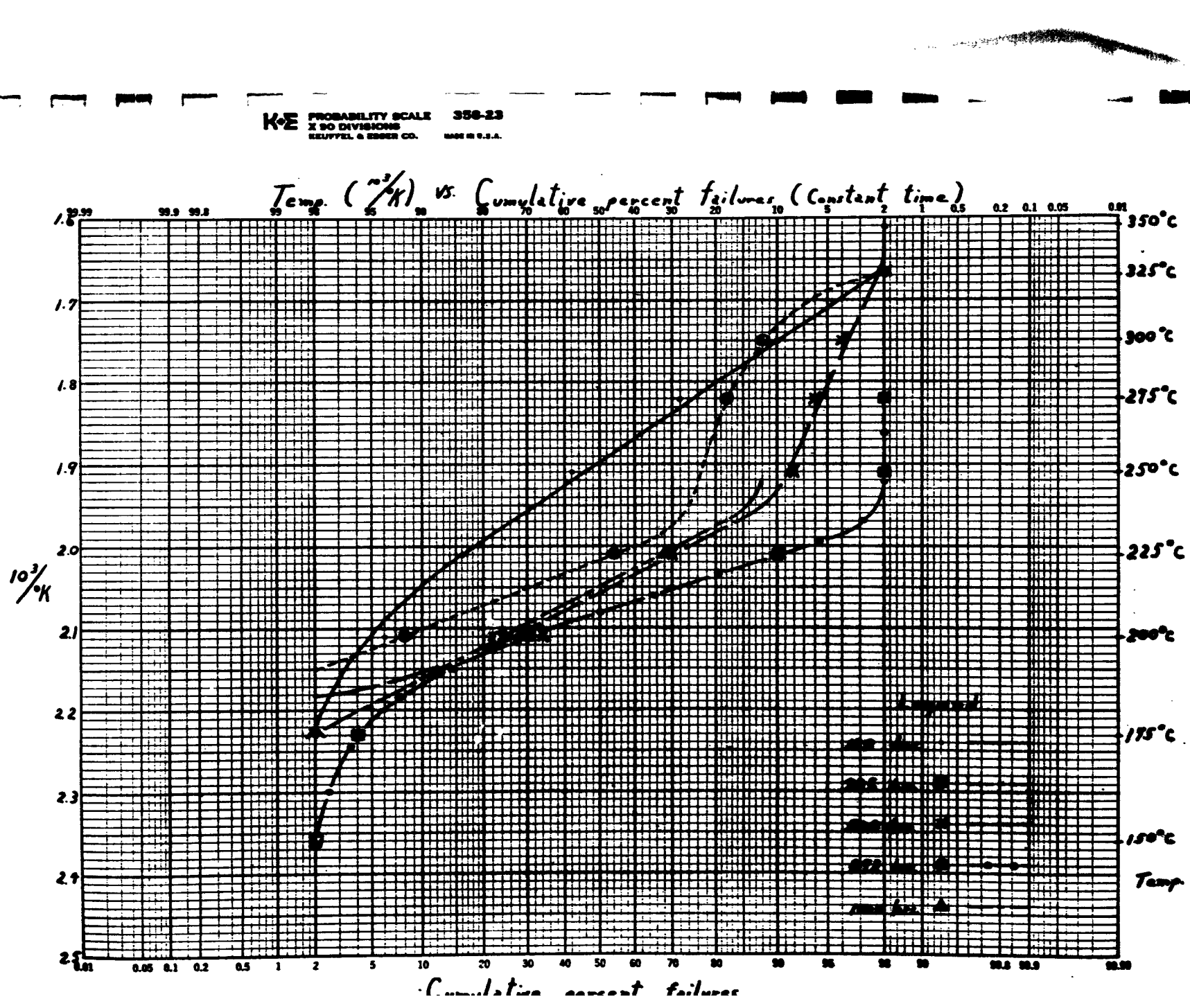
K&E PROBABILITY SCALE 358-23
X 90 DIVISIONS
KEUFFEL & ESSER CO.
Temp. (10^3/°K) vs. Cumulative percent failures (Constant time)
99.99 99.9 99.8 99 98 95 90 80 70 60 50 40 30 20 10 5 2 1 0.5 0.2 0.1 0.05 0.01
1.6 1.7 1.8 1.9 2.0 2.1 2.2 2.3 2.4 2.5
10^3/°K
350°C
325°C
300°C
275°C
250°C
225°C
200°C
175°C
150°C
Temp
0.01 0.05 0.1 0.2 0.5 1 2 5 10 20 30 40 50 60 70 80 90 95 98 99 99.8 99.9 99.99
Cumulative percent failures
-25-

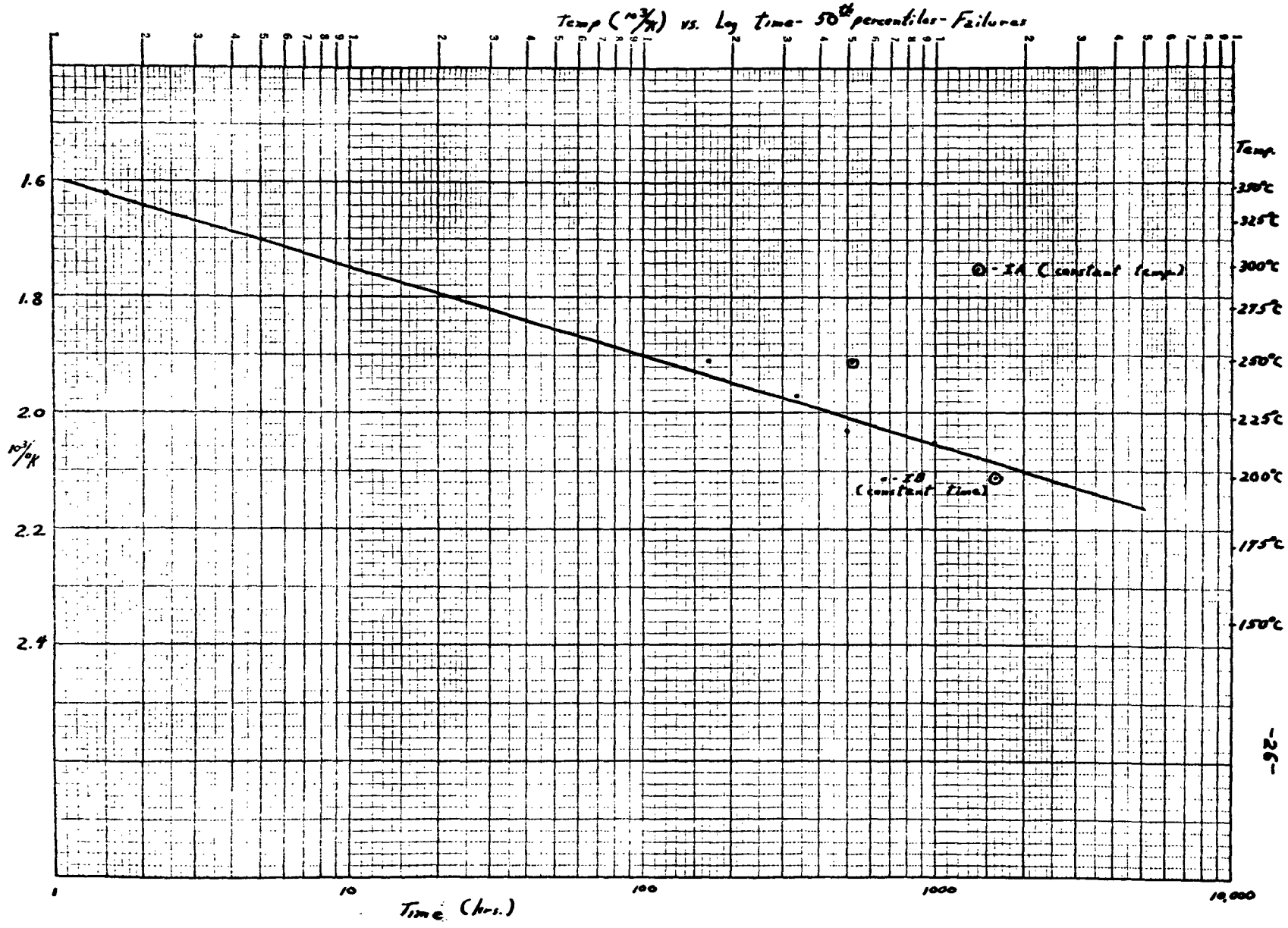
Temp (°K⁻¹/°K) vs. Log time - 50th percentiles - Failures
1.6
1.8
2.0
10³/°K
2.2
2.4
Temp.
350°C
325°C
300°C
275°C
250°C
225°C
200°C
175°C
150°C
⊙ - 1A (constant temp.)
• - 1B (constant time)
1
10
100
1000
10,000
Time (hrs.)
- 126 -

IV. CONCLUSIONS

Several process improvement areas have been essentially completed in this report period. These include material preparation (silicon), material preparation (junction alloy), material preparation (Au-plated Mo), and hard solder assembly. It should be noted that in most cases, development effort has not ceased in the attempt to improve further on these modification, though they have been "finalized" in terms of new process specifications issued for manufacturing. The remaining process improvement phases are progressing satisfactorily and it is expected that, other than the installation of the improved line facility which is a major project in itself, these will be complete as per schedule by the end of the next report period.

The reliability measurements program has continued on schedule.